A Review of BLDC Motor: State of Art, Advanced Control Techniques, and Applications

DEEPAK MOHANRAJ[1], **RANJEEV ARULDAVID**[1], **RAJESH VERMA**[2], **K. SATHIYASEKAR**[3], **ABDULWASA B. BARNAWI**[2], **BHARATIRAJA CHOKKALINGAM**[1], (Senior Member, IEEE), AND **LUCIAN MIHET-POPA**[4], (Senior Member, IEEE)

[1]Department of Electrical and Electronics Engineering, SRM Institute of Science and Technology, Chennai 603203, India
[2]Department of Electrical Engineering, College of Engineering, King Khalid University, Abha 62529, Saudi Arabia
[3]Department of Electronics and Communication Engineering, Prathyusha Engineering College, Chennai 602025, India
[4]Faculty of Engineering, Østfold University College, 1757 Halden, Norway

Corresponding authors: Bharatiraja Chokkalingam (bharatiraja@gmail.com) and Lucian Mihet-Popa (lucian.mihet@hiof.no)

ABSTRACT Brushless direct current (BLDC) motors are mostly preferred for dynamic applications such as automotive industries, pumping industries, and rolling industries. It is predicted that by 2030, BLDC motors will become mainstream of power transmission in industries replacing traditional induction motors. Though the BLDC motors are gaining interest in industrial and commercial applications, the future of BLDC motors faces indispensable concerns and open research challenges. Considering the case of reliability and durability, the BLDC motor fails to yield improved fault tolerance capability, reduced electromagnetic interference, reduced acoustic noise, reduced flux ripple, and reduced torque ripple. To address these issues, closed-loop vector control is a promising methodology for BLDC motors. In the literature survey of the past five years, limited surveys were conducted on BLDC motor controllers and designing. Moreover, vital problems such as comparison between existing vector control schemes, fault tolerance control improvement, reduction in electromagnetic interference in BLDC motor controller, and other issues are not addressed. This encourages the author in conducting this survey of addressing the critical challenges of BLDC motors. Furthermore, comprehensive study on various advanced controls of BLDC motors such as fault tolerance control, Electromagnetic interference reduction, field orientation control (FOC), direct torque control (DTC), current shaping, input voltage control, intelligent control, drive-inverter topology, and its principle of operation in reducing torque ripples are discussed in detail. This paper also discusses BLDC motor history, types of BLDC motor, BLDC motor structure, Mathematical modeling of BLDC and BLDC motor standards for various applications.

INDEX TERMS BLDC motor, torque ripple, current shaping techniques, controlling input voltage, direct torque control, drive-inverter topology, field orientation control, motor design, fault tolerance control, electromagnetic interference reduction.

ABBREVIATION

ANN	Artificial Neural Network.
ASD	Adjustable Speed Drives.
BEMF	Back Electro-Motive Force.
BLDC	Brushless DC Motor.
CF	Cost Function.
DTC	Direct Torque Control.
EMF	Electro Magnetic Field.
EMI	Electromagnetic Interference.
EVs	Electric Vehicles.
FC	Fault Code.
FEA	Finite Element Analysis.
FOC	Field Oriented Control.
FTC	Fault-Tolerant Control.
IEC	International Electrotechnical Commission.
LISN	Line Impedance Stabilization Network.
NdFeB	Neodymium Iron Boron.
NVH	Noise, Vibration, and Harshness.
MPC	Model Predictive Control.

The associate editor coordinating the review of this manuscript and approving it for publication was Ahmed A. Zaki Diab.

PID   Proportional Integral Derivative.
PWM   Pulse Width Modulation.
SVPWM   Space Vector PWM.
VSI   Voltage Source Inverter.
UAV   Unmanned Aerial Vehicle.
ZSI   Z-Source Inverter.

I. INTRODUCTION

A. BACKGROUND

Before 50 years, T. G Wilson and P.H. Trickey conducted several experiments to run Direct Current (DC) motors with solid-state commutation which paved the ideology of developing BLDC motor [1] which is based on Lorentz's force law. In recent decades, BLDC motors have been an area of intensive research to facilitate the penetration of electric vehicles in the automotive industry. Owing to maneuverability, compact design and lightweight BLDC motors are found to be used in several industries such as automotive industries, pumping industries, and rolling industries [2]. Since there will be an increase in demand for electric vehicles in the upcoming 10 years, BLDC motors are expected to play a vital role. The BLDC motors global market is expected to reach a size of 15.2 billion USD by 2025, from an estimated 9.6 billion USD by 2020 as illustrated in Fig. 1. The enormous growth of this machine has lured several applications [3]. Depending on the purpose of applications such as static or dynamic, BLDC motors provide a good response. They need to be designed appropriately to have good magnetic linkage to be used for various applications such as lifting, cutting, and bracing [4]. Compared to the other motors, BLDC motors are expected to have higher efficiency, higher torque to weight ratio, and lower operating noise [5]. These machines have stationary flux in between the rotor and stator which primes the motor to run with a unity power factor. BLDC motors are driven using electronically commutated motor drives. Each phase of the motor is driven via a closed-loop controller. The main usage of a closed-loop controller is to provide a current pulse to the motor windings to have control over the speed and torque as both are complementary phenomena in a motor [6]. BLDC motor is driven with high accuracy that it produces high wear and tear in load conditions.

Few circuits use Hall Effect sensors to directly measure the rotor's position, whereas few others measure the back electromotive force within the non-driven coils to gather the position of the rotor, which are known as sensorless controls. A general hall sensor fixed BLDC motor contains three dual-directional outputs which are controlled by a circuit based on digital logic [7].

Other sensor-less controllers are made for measuring the winding current flow caused by the direction of the magnets to get the position of the rotor and estimating parameters such as back electromotive force (EMF) and flux [8]. Even though indirect control (sensor-less) provides less response compared to direct (with sensor) control and the structural complexity increases, indirect controls are preferred in many high-power automotive applications such as electric
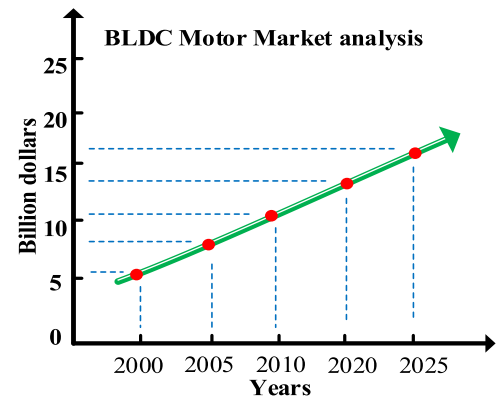

FIGURE 1. BLDC motor market analysis by market reports.

trains, airplanes, etc., Sensor-less control is achieved in three principles namely (i) EMF method with zero-crossing, (ii) observer-based EMF method, and (iii) magnetic anisotropy method [14]. Mostly EMF method with the zero-crossing principle is preferred [9]. While the other two principles are tedious to control and are not preferred for low-speed operations.

For an efficient control, the speed of the motor and the commutation logics are being controlled in the drive-by collecting the inputs from both the drive and the motors such as the position of the rotor or rotor angle, stator currents, hysteresis band current, etc., Proper control of switching of various switches in motor drives confirms the correct rotation of the motor [10]. Even though there are various methods for controlling the harmonic content in the supply in drives, we prefer it to control through the Pulse Width Modulation (PWM) technique [11]. Among the PWM techniques, specifically, everyone prefers to use space vector PWM (SVPWM) control. Current control strategies with PWM and hysteresis controllers play a vital role in improving the performance of the motor drives. Current control strategies with unipolar PWM can be classified as follows: (i) H-PWM-L-ON, (ii) H-ON-L-PWM, ON-PWM, (iii) PWM-ON, (iv) PWM-ON-PWM, (v) H-PWM-L-PWM modes [16].

B. LITERATURE SURVEY AND MOTIVATION

Even though BLDC motors are found to have high efficiency, the durability of the machine is less compared to induction motors [12]. To improve the durability of BLDC motors, the main challenges such as fault tolerance, Electromagnetic interference, acoustic noise, torque ripple, and flux ripple should be controlled. Thus, the controlling techniques are discussed in this paper.

Since BLDC motors are used in dynamic applications, Reliability control techniques of motor drives are indispensable. Reliability control techniques such as fault-tolerant control (FTC), electromagnetic interference control (EMI), and acoustic noise control improve the feasibility of the motor drive systems in dynamic applications. The generation of

TABLE 1. Comprehensive and concise literature survey.

Topology	Adopted techniques	Motor type	Applications	Reliability	Torque ripple mitigation	Ref
Fault-tolerant control (FTC)	Sensory fault tolerance is improved by detecting the fault using discrete Fourier transform.	10 poles 3 phase BLDC	Industrial and commercial applications.	✓	--	[15]
Electromagnetic interference (EMI)	A LISN network is used in such a way that it reduces load parasitic elements.	4 poles 3 phase BLDC	Commercial applications.	✓	--	[16]
Torque ripple reduction using scalar control	Torque ripples are reduced by synthesizing the current wave of power supply.	4 poles 3 phase BLDC	Industry applications.	--	✓	[17]
Torque ripple reduction using vector control	Torque ripples are reduced by using MPC Scheme.	8 poles 3 phase BLDC	Industry applications.	--	✓	[18]
Torque ripple reduction using design topology	Torque ripples are reduced by optimizing the stator and rotor structure.	4 poles 3 phase BLDC	Industry applications.	✓	✓	[19]

EMI and acoustic noises lead to motor failures. Hence, it's essential to control the faults in prior. The various control used to mitigate EMI and acoustic noise generation are discussed. If EMI and acoustic noise lead to the development of fault. The fault-tolerant approach used to work as a backup to continue the operation. The main use of such a technique is to maintain continuity in operations.

In [13] fast fault diagnosis is performed with help of a rapid counter. Whenever the threshold value increases, the fault is detected. The technique is not reliable for high acceleration applications. In [14] EMI of the machine is reduced by analyzing the dc bus voltage at the frequency domain. On analysis, it found that motor structure can improve or decrease the EMI generated. Table 1 represent the comprehensive and concise literature survey done in this paper.

Torque ripples in motors are also mitigated properly by designing the structural symmetry and aligning stator poles in an optimized manner. This results in the reduction of the cogging torque which is one of the main reasons for ripple generation which affects high acoustic noise and EMI interference in the machine itself [20]. The main reason behind the cogging torque generation is the communication between the permanent magnet and stator silicon core [21], [22]. Moreover, concerning the design aspects, the cogging torque ripples are reduced by modifying the magnetic circuit of the machines using various methods such as feedback linearization algorithms, using T-shaped bifurcations teeth in stator slots, closing the slots using a sliding separator, using notches in the rotor of low power motors, concentrating coil winding in the same phase group, reducing claw pole size, magnet step skewing method and U-shaped magnetic poles. These ideologies were performed conventionally to control the torque ripple of the BLDC motor through designing [23], [24]. Every ideology discussed has its disadvantages such as (i) Using modified magnetic circuit reduces torque ripple but results in the increase of additional harmonics, (ii) using T shaped bifurcation teeth in stator slot reduces the mechanical strength of BLDC machines, (iii) introducing notches in the rotor is too difficult, (iv) sliding separators can't be used in

low power machines, (v) concentrating coil winding of the same phase is too difficult, (vi) using magnetic step skewing methodology increases structural complexity of the BLDC machine [25].

Furthermore, vector control techniques such as field orientation control (FOC), direct torque control (DTC), and Model predictive control (MPC) schemes functioned drives are preferred a lot to obtain less torque ripple and good dynamic response over various vigorous conditions. FOC functioned drives were found in the year 1972 and DTC functioned drives were found in the year 1986. During the invention of these techniques, the development of embedded controllers was less [26]. However, the improvement in the development of the embedded controller resulted in the improvement of the steady-state and dynamic response characteristics of the motor controller. The development of various novel computational techniques such as finite control set MPC, intelligent control algorithm, particle swarm optimization, extended Kalman filter algorithm and fuzzy logic estimation functioned drives to improve dynamic response [27]. Therefore, this review article undertakes a comprehensive study on the current research on brushless direct current motor and summarizes the up-to-date technological advancement in BLDC motor drive controls. Furthermore, in this paper the mathematical modeling of motor and motor drives. Reliability control techniques such as EMI filter using LISN techniques, fault-tolerant control using cost observer techniques, and acoustic noise control using field programmable gate array controller are discussed in this paper. The various ideology of FTC is compared. EMI control techniques are compared with suppression levels.

The significant contribution in this paper is as follows:
- A brief history of BLDC motor and their categories are discussed in detail with diagrams.
- A comprehensive review of advanced control techniques such as FTC, EMI control, acoustic noise control, and torque ripple mitigation are discussed.
- The fundamental theory behind BLDC motor designing and its types are illustrated with real-time cases.
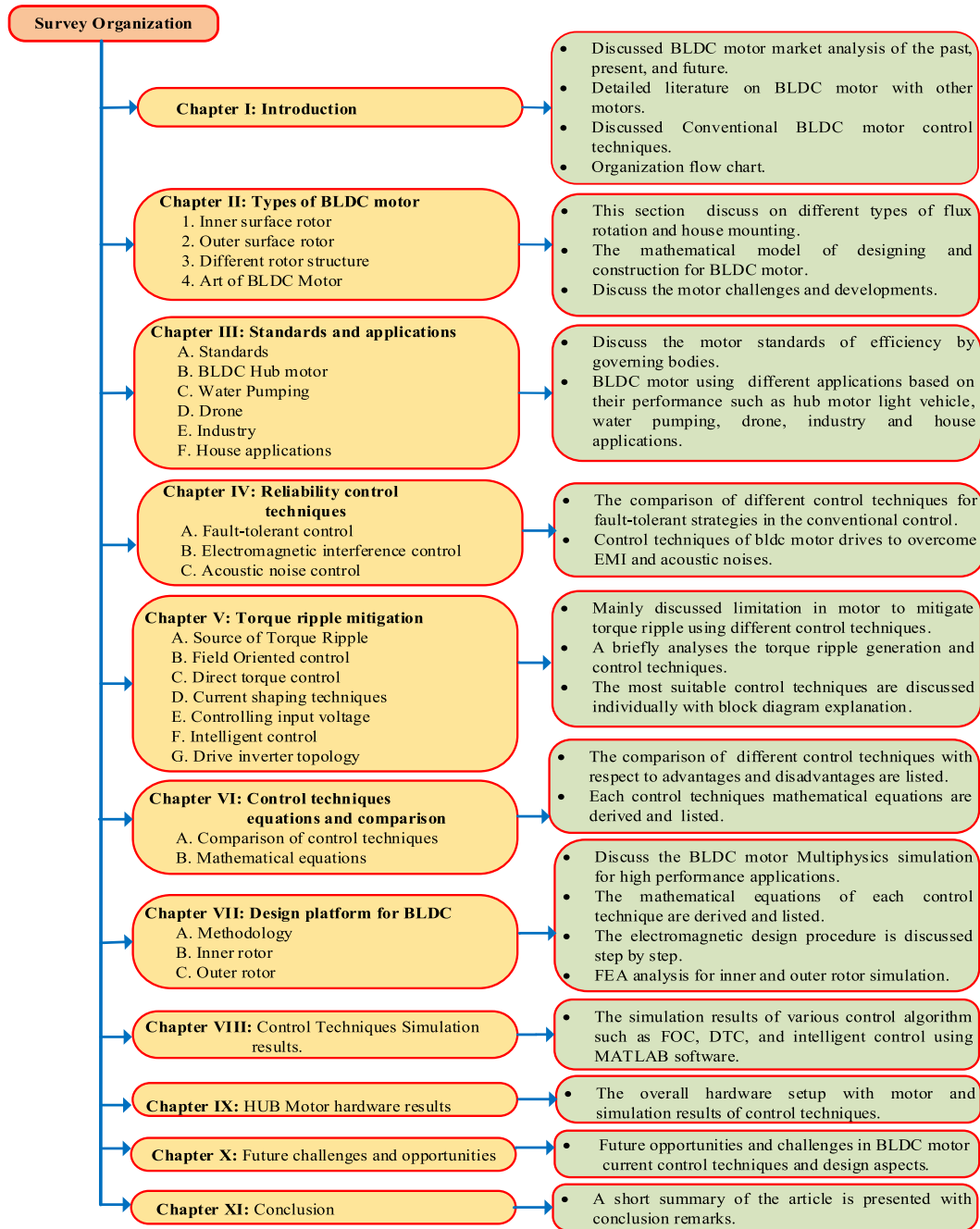
Survey Organization	
Chapter I: Introduction	• Discussed BLDC motor market analysis of the past, present, and future. • Detailed literature on BLDC motor with other motors. • Discussed Conventional BLDC motor control techniques. • Organization flow chart.
Chapter II: Types of BLDC motor 1. Inner surface rotor 2. Outer surface rotor 3. Different rotor structure 4. Art of BLDC Motor	• This section discuss on different types of flux rotation and house mounting. • The mathematical model of designing and construction for BLDC motor. • Discuss the motor challenges and developments.
Chapter III: Standards and applications A. Standards B. BLDC Hub motor C. Water Pumping D. Drone E. Industry F. House applications	• Discuss the motor standards of efficiency by governing bodies. • BLDC motor using different applications based on their performance such as hub motor light vehicle, water pumping, drone, industry and house applications.
Chapter IV: Reliability control techniques A. Fault-tolerant control B. Electromagnetic interference control C. Acoustic noise control	• The comparison of different control techniques for fault-tolerant strategies in the conventional control. • Control techniques of bldc motor drives to overcome EMI and acoustic noises.
Chapter V: Torque ripple mitigation A. Source of Torque Ripple B. Field Oriented control C. Direct torque control D. Current shaping techniques E. Controlling input voltage F. Intelligent control G. Drive inverter topology	• Mainly discussed limitation in motor to mitigate torque ripple using different control techniques. • A briefly analyses the torque ripple generation and control techniques. • The most suitable control techniques are discussed individually with block diagram explanation.
Chapter VI: Control techniques equations and comparison A. Comparison of control techniques B. Mathematical equations	• The comparison of different control techniques with respect to advantages and disadvantages are listed. • Each control techniques mathematical equations are derived and listed.
Chapter VII: Design platform for BLDC A. Methodology B. Inner rotor C. Outer rotor	• Discuss the BLDC motor Multiphysics simulation for high performance applications. • The mathematical equations of each control technique are derived and listed. • The electromagnetic design procedure is discussed step by step. • FEA analysis for inner and outer rotor simulation.
Chapter VIII: Control Techniques Simulation results.	• The simulation results of various control algorithm such as FOC, DTC, and intelligent control using MATLAB software.
Chapter IX: HUB Motor hardware results	• The overall hardware setup with motor and simulation results of control techniques.
Chapter X: Future challenges and opportunities	• Future opportunities and challenges in BLDC motor current control techniques and design aspects.
Chapter XI: Conclusion	• A short summary of the article is presented with conclusion remarks.

FIGURE 2. Organization flow chart.

• The simulation and designing of advanced motor controls are discussed in detail.
• The open challenges and future research opportunities are discussed.

Fig. 2. represents the flow and survey organization of the presented paper. In the next section, the various types of BLDC motors and state of art are discussed.

II. TYPES OF BLDC MOTOR

BLDC motor physical design is divided into two parts stator and rotor. The classification of BLDC motor types is shown in Fig. 4. The motor is constructed with various configurations such as inner rotor and outer rotor. In [28] the outer rotor-designed BLDC motor is discussed. The rotor permanent magnet is embedded at the outer surface and stator windings are kept stationary inside. The outer rotor BLDC increases the output torque and power density of the motor.

The outer rotor BLDC motor is mainly used in electric vehicles, drones, variable drive industries, water pumping, and home electronics. In [29] outer rotor BLDC motor is designed, the airgap radius between stator and rotor is minimized. Thus, increasing the torque capability per unit length and current. In [30] structural elements are added to increase the stability of the rotor. These improve motor characteristics
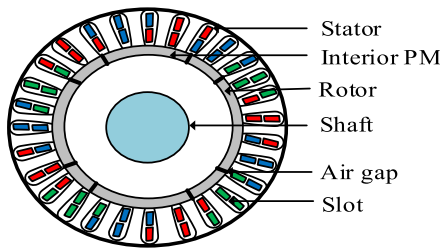
FIGURE 3. Inner rotor.

TABLE 2. Comparison of the inner and outer rotor features.

BLDC motor physical design	Inner Rotor	Outer rotor
Stator	• Iron less core stator winding outside.	• Iron cored stator winding inside.
Speed	• High-speed motors are available.	• Low and medium speed motor available.
Inertia	• Low inertia	• High inertia
Noise	• Quickly changing direction makes noisy.	• Noise less.
Maintenance	• Less maintenance.	• High maintenance.
Efficiency	• High efficiency.	• Less efficiency compares to the inner rotor.
Torque	• Minimum torque.	• Produce more torque.
Power to weight ratio	• Compare to outer run less.	• High.
Gear box	• Gear box required.	• No gear box required.
Advantage	• Rotating shaft moment of inertia is small. • Heat dissipation efficiency high. • Reduce the downsize unit. • Compact size. • High output power.	• Increasing the torque capability and current. • Reducing heat dissipation. • Low cogging force. • Large airgap. • Increase torque.
Disadvantage	• Requires high magnetic flux density. • Need high-performance magnet. • High cogging force.	• Complex to design rotor embedded with magnets. • Mechanical stability. • Cooling stator winding.

in dynamic conditions. Fig. 5 depicts the outer rotor-type BLDC motor. In [31] inner rotor BLDC motor designing is discussed. Using finite element analysis, the ferrite bonded magnet used BLDC motor is analyzed.

On experimentation, it found that the inner rotor motor also provides good power characteristics over dynamic conditions. In [32] preliminary algorithm of high-speed ferrite-based BLDC motor is discussed. Magnetic flux components are improvised by adjusting the mechanical constraints. Fig. 3 represents the inner rotor BLDC motor structures. The comparison of the inner rotor and outer rotor BLDC is discussed in Table 2.

Depending on the construction of the PM rotor, rotors in BLDC motor usually consist of permanent magnets and a shaft. The cross-section of permanent magnets in motors can be classified into various types such as (i) surface mounted magnet [33], (ii) inserted magnet [34], and (iii) buried or embedded type rotor magnets [35], [36]. In this, the buried or embedded type has more efficiency compared to other types. Table 3 compares the various permanent magnet rotor structures of the BLDC motor.

Depending on the expectation of the customers, these BLDC motor drives are integrated in different ways such as magnetic field path radial and axial flux. Axial flux motors
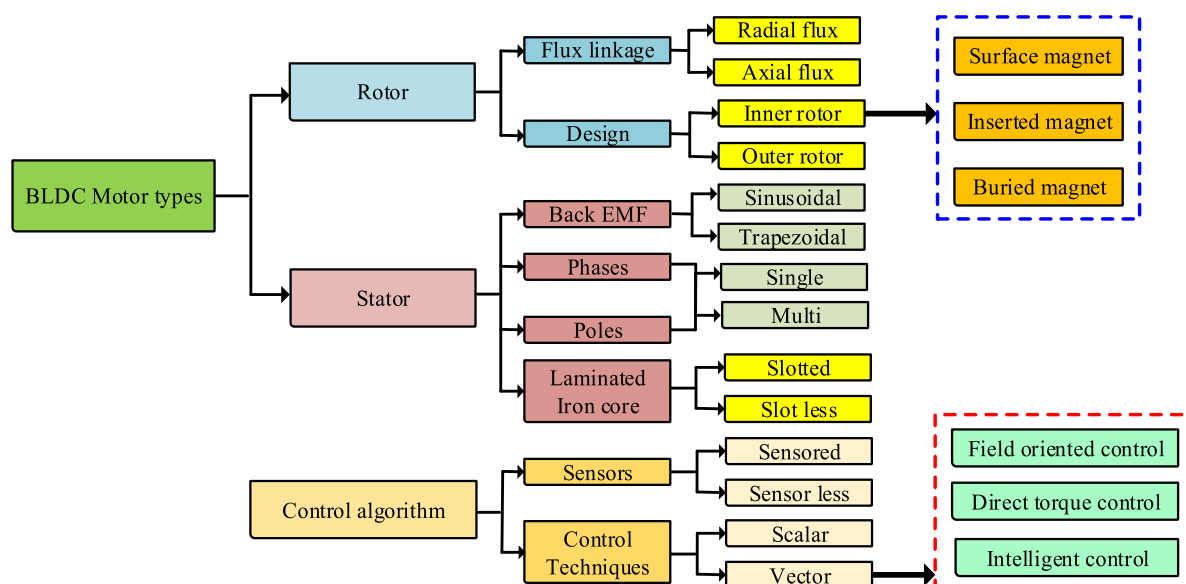
FIGURE 4. Types of BLDC motor and control algorithms.

TABLE 3. Comparison of the various permanent magnet rotor structure.

Content	Surface magnet	Inserted magnet	Buried magnet
PM rotor structure			
Torque/weight ratio	• Very good.	• Very good.	• Very good.
High-speed running capability	• Less preferred for high-speed operation.	• Compared to surface mounted it has a good affinity towards high-speed operations.	• It shows the best performance at high speed.
Power factor	• Power factor obtained is less.	• Power factor obtained is less.	• Power factor obtained is good.
Efficiency	• Less compared to buried.	• Less compared to buried type.	• Very high compared to the other types.
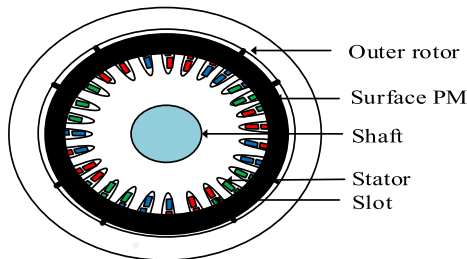
FIGURE 5. Outer rotor (Hub motor).
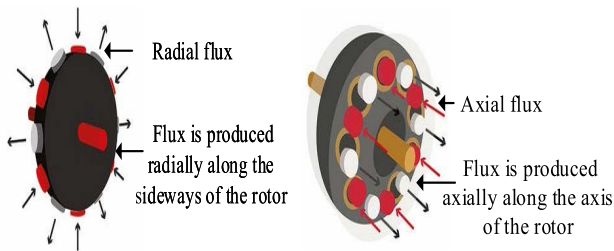
FIGURE 6. Radial and axial flux.

TABLE 4. Electromagnetic axial and radial flux path difference.

Magnetic flux direction	Axial flux	Radial flux
Flux direction strength	• Flux-path is shorter.	• Flux-path is longer.
Magnetic field	• Strong	• weak
Efficiency	• High	• Compare to axial low.
Power density	• High	• Minimum.
Direction	• Flux unidirectional path.	• 2D dimensional path.
Iron loss	• Decreasing iron loss.	• Iron loss maximum.
winding	• Minimum heat conductivity.	• Low thermal conductivity.
diameter	• High	• Medium
Active length	• Minimum	• High
Mass	• Low	• High
Output voltage	• High	• Low.
Outer rotor	• High torque.	• Less torque.

are more powerful than radial flux motors. In [37] the characteristics of axial flux type BLDC motor are analyzed using flux linkage methodology. The mechanical stability of the BLDC motor is improved by the dual rotor technique.

In [38] three different types of radial flux motors are compared and analyzed. On analysis, it's found that dual rotor type produces good dynamic characteristics. The axial flux and radial flux features are compared in Table 4. Fig. 6 represents the axial and radial flux motor flux linkages flow.

Further, BLDC motor classification based on stator components is discussed. The stator in BLDC can be classified based on the number of phases, laminated core types, and back EMF. The stator in BLDC can be classified based on the number of phases of operation. In static applications, mostly

single-phase and three-phase motors are used. Three-phase, five-phase, and seven-phase motors are preferred for dynamic applications such as electric vehicles. In [39] multiphase BLDC motor is designed with the help overlapping winding strategy. Using an overlapping strategy provides better flux linkage between the coils. Multiphase motor topologies provide good torque characteristics and improved fault tolerance capability. The stator coil winding is star or delta connected. These winding models are preferred depending upon the application. Star connection is preferred for high torque low-speed applications and delta connection is preferred for low torque low-speed applications. Depending on the speed, the number of poles in the rotor is increased.

The laminated iron cores are classified as slotted and slotless cores. In [40] due to the reaction of the PM flux with the stator's varying permeance, the slotted stator often generates high-order spatial harmonics. This causes a small vibrating

TABLE 5. BLDC stator slotted and slotless structure features.

Stator structure	Slotted	Slotless
Advantages	• Uneven magnetic pull. • High power density. • Higher order spatial harmonics. • Easier to protect.	• High power density. • Low cogging torque • Better overload capacity. • Limit the operational noise. • Increase operating frequency.
Disadvantages	• Volume of the machine size is big. • Poor overloading. • High cogging torque. • Enables to operate at high speed. • Less efficiency. • Increasing noise and vibration.	• Low inductance to control motor is challenging. • Not suitable for harsh environmental conditions.

torque on the shaft, which is referred to as cogging torque. As a result, it reduces operational noise preferred for slotless machines. Furthermore, slot-less machines have lower rotational eddy loss, allowing the motor to run at faster speeds. Features of slotted and slotless are compared in Table 5.

The stators are also further classified based on their back emf waveforms which are sinusoidal waveform and trapezoidal waveform. The back emf shape depends on the interconnection between the stator windings and the air gap distance. BLDC motor is more efficient for sinusoidal back emf compared to trapezoidal back emf. These motors are a little bit costlier due to the use of more copper windings compared to trapezoidal back EMF BLDC motors [39]–[41].

Mathematical modeling of BLDC motors is needed for designing and constructing BLDC motors. The mathematical modeling of BLDC motors is discussed in detail. The position of the BLDC motor can be estimated by designing the model of a conventional DC motor which can be represented by winding resistance, the inductance of the winding coils, and the back electromotive force [41].

A three-phase BLDC motor has three individual phase windings and a permanent magnet rotor. Modeling rotor-induced currents are neglected due to the high resistivity of magnets and silicon core [42].

The three-phase voltage equations for windings are modeled as follows,

$$\begin{bmatrix} v_x \\ v_y \\ v_z \end{bmatrix} = \begin{bmatrix} R & 0 & 0 \\ 0 & R & 0 \\ 0 & 0 & R \end{bmatrix} \begin{bmatrix} i_a \\ i_b \\ i_c \end{bmatrix} + \frac{d}{dt} \times \begin{bmatrix} L_{aa} & L_{ab} & L_{ac} \\ L_{ba} & L_{bb} & L_{bc} \\ L_{ca} & L_{cb} & L_{cc} \end{bmatrix} \begin{bmatrix} i_a \\ i_b \\ i_c \end{bmatrix} + \begin{bmatrix} e_a \\ e_b \\ e_c \end{bmatrix} \quad (1)$$

where v_x, v_y, and v_z are phase voltages of the BLDC motor, R is the stator resistance of the BLDC motor, i_a, i_b and i_c are the stator currents of the BLDC motor, L_{aa}, L_{bb} and L_{cc} represent the stator inductance of the BLDC motor, e_a, e_b, and e_c represent the back EMF of the BLDC motor. The resistance of the machine is assumed to be equal.

The reluctance between the stator and rotor are assumed to be null (i.e., there is no change in the stator and rotor reluctance angle.) then,

$$L_{aa} = L_{bb} = L_{cc} = L \quad (2)$$

$$L_{ab} = L_{ac} = L_{ba} = L_{ca} = L_{cb} = L_{bc} = M \quad (3)$$

Substituting the above equations in equation (1),

$$\begin{bmatrix} V_x \\ V_y \\ V_z \end{bmatrix} = \begin{bmatrix} R & 0 & 0 \\ 0 & R & 0 \\ 0 & 0 & R \end{bmatrix} \begin{bmatrix} i_a \\ i_b \\ i_c \end{bmatrix} + \frac{d}{dt} \times \begin{bmatrix} L & M & M \\ M & L & M \\ M & M & L \end{bmatrix} \begin{bmatrix} i_a \\ i_b \\ i_c \end{bmatrix} + \begin{bmatrix} e_a \\ e_b \\ e_c \end{bmatrix} \quad (4)$$

Since the motor is star connected. The stator currents are considered to be balanced.

$$i_a + i_b + i_c = 0 \quad (5)$$

This is used to simplify the inductance matrix as,

$$Mi_b + Mi_c = -Mi_a \quad (6)$$

Therefore, the main equation becomes,

$$\begin{bmatrix} V_x \\ V_y \\ V_z \end{bmatrix} = \begin{bmatrix} R & 0 & 0 \\ 0 & R & 0 \\ 0 & 0 & R \end{bmatrix} \begin{bmatrix} i_a \\ i_b \\ i_c \end{bmatrix} + \frac{d}{dt} \times \begin{bmatrix} L-M & 0 & 0 \\ 0 & L-M & 0 \\ 0 & 0 & L-M \end{bmatrix} \begin{bmatrix} i_a \\ i_b \\ i_c \end{bmatrix} + \begin{bmatrix} e_a \\ e_b \\ e_c \end{bmatrix} \quad (7)$$

Since the back EMF of BLDC motor is trapezoidal. The back EMF equations are given as,

$$\begin{bmatrix} e_a \\ e_b \\ e_c \end{bmatrix} = \omega_m \lambda_m \begin{bmatrix} f_{as}(\theta_r) \\ f_{bs}(\theta_r) \\ f_{cs}(\theta_r) \end{bmatrix} \quad (8)$$

where ω_m the rotating speed of the motor, λ_m is the flux linkage of the motor $f_{as}(\theta_r), f_{bs}(\theta_r)$ and $f_{cs}(\theta_r)$ represents the functions of back EMF for various magnitude instants. The flux linkages between the stator and rotor are made smooth.

Hence the electromagnetic torque developed by the BLDC motor is given by the following expression:

$$T_e = \frac{1}{\omega_m} * (e_a i_a + e_b i_b + e_c i_c) \quad (9)$$

The obtained phase voltage equation looks similar to the armature voltage equation of the direct current machine. The equation of motion of motor drive,

$$T_e - T_m = J \frac{d\omega}{dt} + F\omega(t) \quad (10)$$

where J is the combined inertia, F is the mechanical friction co-efficient. Mechanical speed of the motor is related by,

$$P\omega_m = \frac{d\theta_r}{dt} \quad (11)$$
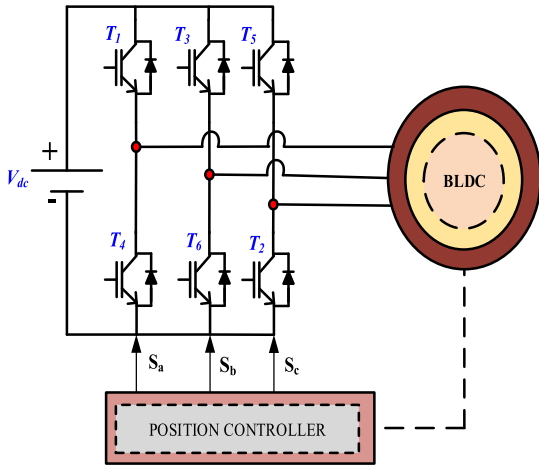
where P is the number of poles of the motor.

FIGURE 7. The power circuit of scalar control of BLDC motor.

FIGURE 8. BLDC axial flux integrated inverter mounted [159].

Combining all the relevant equations, the system in state-space equation becomes,

$$x = Ax + Bu + Ce \quad (12)$$

Were,

$$x = \begin{bmatrix} i_a & i_b & i_c & \omega_m & \theta_r \end{bmatrix} \quad (13)$$

$$A = \begin{bmatrix} -\dfrac{R}{L-M} & 0 & 0 & -\lambda_m f_{as}(\theta_r) & 0 \\ 0 & -\dfrac{R}{L-M} & 0 & -\lambda_m f_{bs}(\theta_r) & 0 \\ 0 & 0 & -\dfrac{R}{L-M} & -\lambda_m f_{cs}(\theta_r) & 0 \\ \lambda_m f_{as}(\theta_r) & \lambda_m f_{bs}(\theta_r) & \lambda_m f_{cs}(\theta_r) & -\dfrac{B}{J} & 0 \\ 0 & 0 & 0 & \dfrac{P}{2} & 0 \end{bmatrix} \quad (14)$$

$$B = \begin{bmatrix} \dfrac{1}{L-M} & 0 & 0 & 0 \\ 0 & \dfrac{1}{L-M} & 0 & 0 \\ 0 & 0 & \dfrac{1}{L-M} & 0 \\ 0 & 0 & 0 & \dfrac{1}{L-M} \end{bmatrix} \quad (15)$$

$$C = \begin{bmatrix} -\dfrac{1}{L-M} & 0 & 0 \\ 0 & -\dfrac{1}{L-M} & 0 \\ 0 & 0 & -\dfrac{1}{L-M} \end{bmatrix} \quad (16)$$

The BLDC motor operates with Quasi-sinusoidal phase current and trapezoidal back EMF provided by the rotor switching table from Table 6.

Fig. 7 depicts the power circuit for the scalar control of the BLDC motor [43]. The power switches (T_1 to T_6) are IGBT devices and are controlled by PWM signals (S_a, S_b, S_c).

With the above setup, the BLDC motor can also be clubbed together in the future. Hence the motor transmission losses
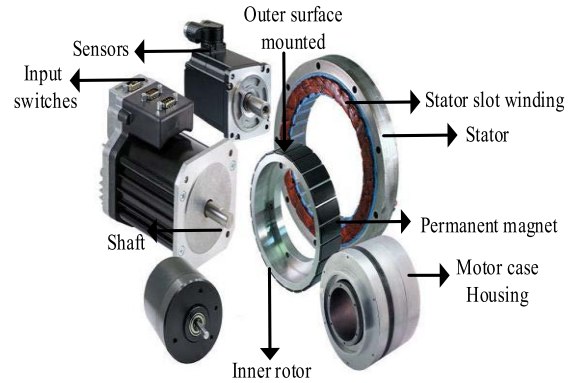
are reduced [44], [45]. The motor drive systems are classified as (i) Radially housing mounted, (ii) Radially stator iron mounted, (iii) Axially housing mounted, (iv) Axially stator iron mounted. The integrated motor drive figure is depicted in Fig. 8.

While reviewing the types and structure of BLDC motors, various technical challenges that need to be considered while designing and constructing BLDC motors are discussed.

A. REDUCED MASS
The designed motor should have less weight. The designed motor may be used for various applications such as traction, pumping, household, etc. Depending on the purpose, the designed motor weight may vary but a motor with less weight can be used for various applications. Reduced mass is much related to reducing volume. For applications such as hand tools, the motor used requires high power and reduced volume. Hence, the designed motor should be of small size [46].

B. HIGH EFFICIENCY
The main purpose of migrating from a conventional motor system (i.e., induction motor) to a BLDC motor is for improving the competence of the system. This is achieved by designing a motor with less torque ripple, improved flux linkage, and thermal stability of the system [64].

C. LOW COST
Usually BLDC motors run with motor drives. These drives may be integrated or kept separately. Motors and motor drives are usually very high in cost. Keeping a drive separately may increase the installation cost using wiring cables, individual wiring, etc., Cost reduction in motor design is done using various component materials while manufacturing [47].

D. IMPROVED FAULT TOLERANCE
While designing a BLDC motor, it is very much necessary to detect the rotor position for providing the commutation in power switches. These rotor position detectors are hall sensors, speed sensors, stator flux coils, etc. In heavy applications such as electrical vehicle tractions, it is very difficult

TABLE 6. Switching operation for scalar control of BLDC motor.

Step	Rotor Position Signal	Reference Currents			Hall Sensor output			Switch ON position	Switch OFF position	Controlled Switch
	θ_r	i_a*	i_b*	i_c*	H_a	H_b	H_c			
1	0°-60°	1	0	-1	1	0	0	T_1	T_3, T_4, T_5, T_6	T_2
2	60°-120°	0	1	-1	1	1	0	T_2	T_1, T_4, T_5, T_6	T_3
3	120°-180°	-1	1	0	0	1	0	T_3	T_1, T_2, T_5, T_6	T_4
4	180°-240°	-1	0	1	0	1	1	T_4	T_1, T_2, T_3, T_6	T_5
5	240°-300°	0	-1	1	0	0	1	T_5	T_1, T_2, T_3, T_4	T_6
6	300°-360°	1	1	0	1	0	1	T_6	T_2, T_3, T_4, T_5	T_1

to continue the operation if there is any fault in the rotor position sensors. Hence, it is very necessary to improve the fault tolerance of the motor [48].

E. IMPROVED THERMAL STABILITY

Technologies must be developed which is very useful in improving the thermal stability of the system. Thermal stability can be improved by using winding materials with less resistance, stator core with high flux linkage, and interior permanent magnet with high flux linkage. In certain cases, the thermal stability can also be improved by improving the cooling system. In some static scenarios, motor drive systems are integrated with motors which may lead the motor to operate in high temperatures. Hence, proper cooling must be provided to the system [49].

F. LESS NOISE

The acoustic noise generation in BLDC motor is due to the electromagnetic forces, structural design, and odd harmonics development in the motor windings. A good BLDC machine has fewer acoustic noises developed. This can be reduced by skewing rotor and stator slots incorrect angles, and commutating power switch at the correct instant [50].

G. HIGH VIBRATION

In the general case, whenever a motor is operated by drives there will be the generation of common-mode voltages in the cable which connects drive and motor and bearing currents in the yoke of the motor. This leads to frosting, spark tracks on the bearing. Hence, the motor also experiences more vibration. This can be reduced by the proper grounding of devices using dv/dt filters, and electromagnetic interference (EMI) filters [50].

H. REDUCTION IN POWER ELECTRONICS COST

Usage of power electronics drives in industry or household purposes may lead to an increase in the overall expense of the system. These motor drives may be integrated with motors or kept separated. The cost reduction depends on major factors such as materials, manufacturing process, standardization, and modularization [51]. Owing to the various challenges and state of art of BLDC motors, the various applications and

global standards of BLDC motors are reviewed in the next section.

III. STANDARDS AND APPLICATIONS

A. STANDARDS

The efficiency of the system is one of the key factors to improve the feasibility of a product.

Standards of efficiency for motors are set and given by governing bodies of that particular region such as the International Electro-technical Commission (IEC) in Europe and the National Electrical Manufacturers Association (NEMA) in the United States of America. Present IEC motor standards have four levels [50].

These IEC 60034-30-1 efficiency classes are categorized into four are the following

1. IE1 (standard efficiency)
2. IE2 (high efficiency)
3. IE3 (premium efficiency)
4. IE4 (super premium efficiency)

The Standard given to the motor defines the efficiency of either a 50 Hz or a 60 Hz motor drive with a single-phase winding or three-phase windings built with the BLDC motor drive with an output power higher than 120W [52].

National Electrical Manufacturers Association (NEMA) of the United States of America has provided the guidelines for motor efficiency standards. The standards are classified as,

1. Old Standard Efficiency Motor
2. Prior NEMA EE
3. NEMA Energy
4. NEMA Premium

Like the International Electro-technical Commission standards, the NEMA requirements for efficiency also increase with higher output power. For most of the standards, the assumptions are made in such a way that each motor drive is manufactured and optimized for a specific application with different sectors as shown in Fig. 9. In this section, we are reviewing the various standards of BLDC motors in various applications [53].

Both inner and outer rotor-based BLDC motors are used in diverse applications due to their advantages of high torque-weight ratio, compact size, etc. However, depending upon the required speed of less than 500rpm, 501 to 2000 rpm, 2001 to
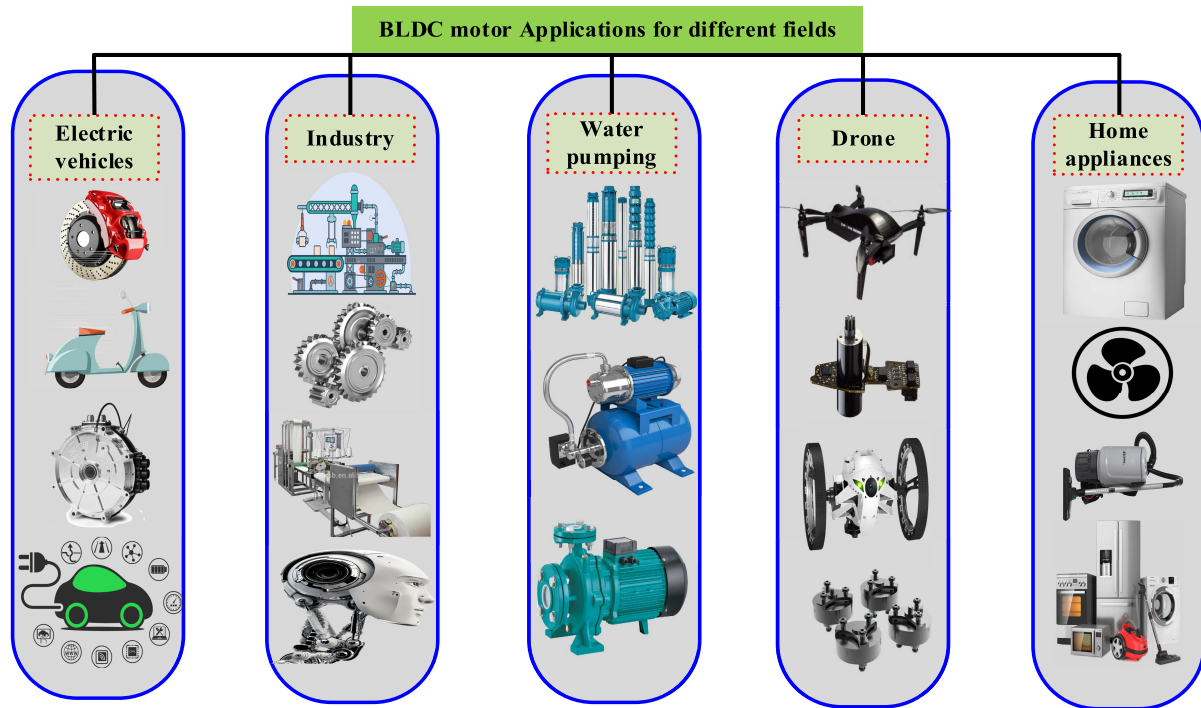
FIGURE 9. Applications of BLDC motors in diverse sector.

10000rpm, and above 1000rpm, the BLDC motor types are selected for specific applications.

B. ELECTRIC VEHICLE

By exploring several countries and their development in electric vehicle transformation, during the first half of the decade, electric vehicle sales were soaring. By now more than 10 million electric vehicles are on the road. In this 47% of the vehicles are only from China. Similarly in several countries, more than 1% of its market share is contributed towards electric vehicles. BLDC motors are preferred for lightweight electric vehicles. Especially BLDC hub motors are used in electric scooters due to the advantage of retrofitting. BLDC hub motors are driven using both sensor and sensor-less motor controllers. In [54] using hub motors in lightweight electric vehicles improves the Back EMF by 3%. The main disadvantage of using hub motors is (i) increases the weight at the power-driven side which decreases the vehicle stability, (ii) Delivering uniform torque is too difficult and (iii) Mechanical stress experienced by hub motors is more compared to normal BLDC motor. IE-2, IE-3, or IE-4 efficiency standards-based BLDC motors are used in EVs. Fig. 10 shows the BLDC hub motor structure and its subparts. The motor controller specifications are not standardized till now, several manufacturers produce two-wheeler electric vehicles of their customized standards such as operating voltage 24 V and 48 V battery power from 40Ah-100Ah, motor power till 6 kW. BLDC motors are not only preferred for power transmission in electric vehicles. We can use BLDC motors for applications such as turbochargers, blowers, seat

comforting systems, etc., [55]. Table 7 shows a comparison of several electric vehicles and their power rating and power train drive type, operating voltage, power, and battery used across the world.

Increased fault tolerance capability, reduced EMI and reduced torque and flux ripples increase the reliability of the BLDC motor in the EV application. In electric vehicles, the conducted emission sources are characterized in a particular frequency which leads to distortion of the system. In [56] the EMI sources which are spread through cables, and their mitigation method are discussed. Power cables generate more EMI due to conductive sources and mismatching frequencies. These EMI are mitigated by predicting distributed element parameters at the resonant frequency of the system. This improves the reliability of BLDC motor systems. Similarly, improving fault tolerance capability also increases the reliability of the system. In [57] a time-efficient fault detection algorithm for BLDC, motors in electric vehicles applications are discussed. When BLDC motors are subjected to fault conditions, the speed of the machine fluctuates instead of being constant, the back EMF of the machine also varies, and change in phase sequence leads to stator faults. Thus, the fault conditions are detected. The efficient FTC is performed by model-based techniques which are discussed in detail in a further section. Torque ripples in BLDC motors in EV applications effects shaft failures, increased vibrations, and acoustic noises. In [58] torque ripples and flux ripples are reduced by using the DTC algorithm which reduces stator iron losses using compensation and improves torque per ampere of the machine.

TABLE 7. BLDC motor specifications for EVs in different ranges from India, China, the U.K., and the USA.

EV Model	Country	Operating Voltage (Volt)	Battery type	Power (kW)	Motor	Drive	Year
22 Motors, NDS Eco Motors	India	72	Li-ion	2.1,1.5	BLDC	Hub motor	2015
Ather 340	India	48	Li-ion	3.3	BLDC	Hub motor	2018
Ather 450	India	48	Li-ion	5.4	BLDC	Hub motor	2018
Bajaj chetak	India	48	Li ion	4	BLDC	Hub motor	2020
Hero electric A2B	India	36	Li-ion	0.5	BLDC	Hub motor	2021
Revolt RV400	India	72	Li-ion	4	BLDC	Mid-drive	2019
TVS I qube	India	48	Li-ion	4.4	BLDC	Hub motor	2020
Hero Electric flash	India	48	Li-ion	0.25	BLDC	Hub motor	2021
Detel EV Easy plus	India	48	Li-ion	0.25	BLDC	Hub motor	2021
Pure EV Pluto	India	48	Li-ion	2.2	BLDC	Hub motor	2020
Aima E Light Scooter	China	48	Lead-acid	0.5	BLDC	Hub motor	2020
Artisan es-1 pro	United Kingdom	72	Li-ion	11	Advanced PM	Mid-drive	2020
Artisan ev0	United Kingdom	72	Li-ion	3	Advanced PM	Mid-drive	2019
Harley Davidson Livewire	USA	12	Li-ion	78	Advanced PM	Mid-drive	2019
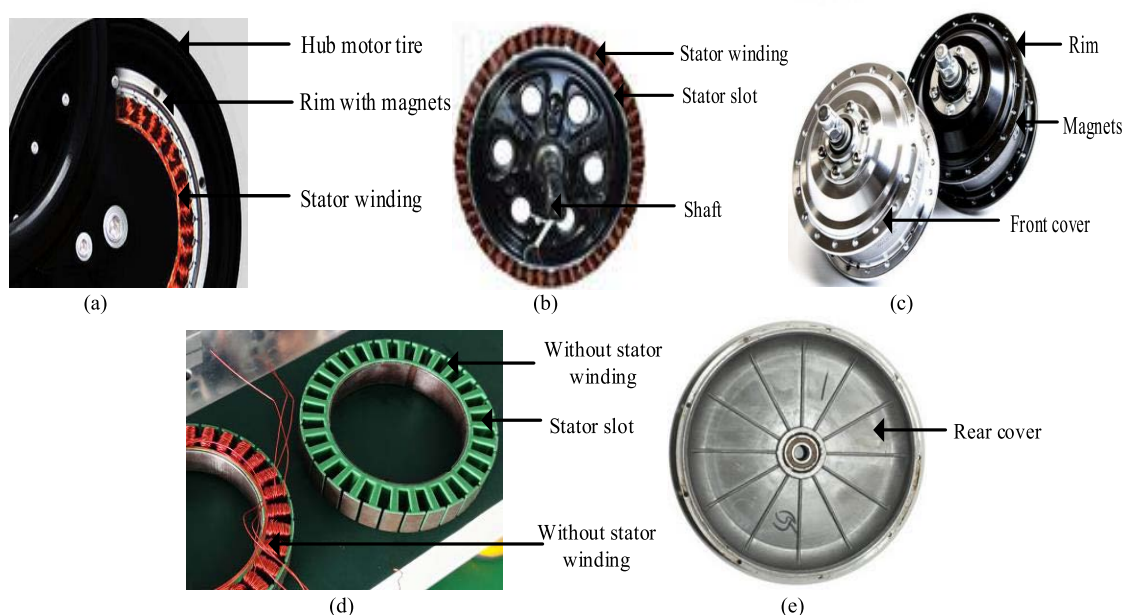
FIGURE 10. (a) Hub motor structure. (b) Stator winding Connection. (c) Tire rim. (d) Without stator winding. (e) Motor rear cover.

In the future, multi-motor concepts are given special importance in electric vehicle applications. Hence, the BLDC motor-driven electric vehicles with four motors at each wheel are discussed in this paper. The advantages and disadvantages of multi-motor concepts are also discussed. In [59] electric cars are driven using four hub wheel motors is discussed. Driving hub motor at low speed increases the acoustic noises. Hence, EVs of multi motoring concept drive with huge noise. Acoustic noises are reduced by using a vector control algorithm which benefits in the reduction of torque ripple and acoustic noises.

Hence, EVs of multi motoring concept drive with huge noise. Acoustic noises are reduced by using a vector control algorithm. In multi motor-driven EVs, Regenerative braking affects more energy storage compared to single motor-driven EVs. In [60] the e-differential technique will be based on Ackerman-Jeantaud geometry. Fig. 11. depicts the block diagram of electrical differential for a multidrive system.
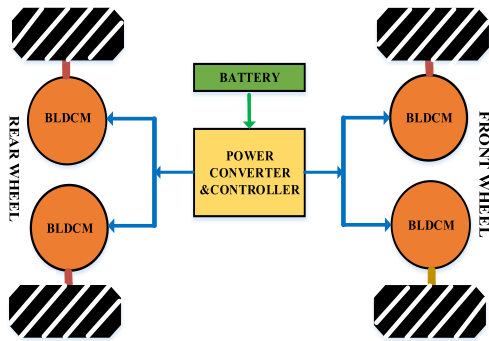
FIGURE 11. Block diagram of electrical differential for electric vehicle.

FIGURE 12. Submersible pump motor model.

C. WATER PUMPING

BLDC motors are preferred for pumping applications due to their nature of saving energy. The standards are preferred depending upon the power ranges. IE-1 is preferred for low-power pumping applications. IE-2 and IE-3 are preferred for mid and high-power applications. For efficient usage, these BLDC motors are integrated with renewable energy sources such as solar energy. In [61] a water pumping system electrified using a photovoltaic system is employed. To obtain the maximum amount of energy from the solar board. Zeta converter, maximum power point tracking is engaged. These applications are tested for various dynamic conditions. Since the converter is operated in continuous current mode, various stresses in switches are reduced on its components. The MPPT (maximum power point tracking) is designed using a PI controller in such a way that it avoids perturbation in the systems. On driving through solar panels, torque ripples are reduced by maintaining the solar output voltage constant. In [62] a pumping system, electrified using solar power is discussed. When solar power is not used for water pumping, excessive power is connected to the grid for the utilization of people.

The motor is operated through a three-phase drive and is connected to a single-phase grid. To control the voltage source inverter in both directions (supply-side and grid side), a single phase-phase locked loop control is used. In addition to this in [63], the power flow control in the grid is discussed. The power flow control is done using a boost converter. In [64] a method of controlling solar panels without a DC-DC converter is discussed in solar water pumping applications. A diode is connected in series to avoid the reverse flow of current. The MPPT is controlled using the voltages and current obtained from the motor side. The motor signals are converted as the desired signal for MPPT using a saw-tooth converter. Hence, using the BLDC motor in water pumping applications not only increases efficiency but also helps in the efficient cost of productivity. Fig. 12. represents the motor model of the BLDC motor used in a water pump application.

In [65], [66] the design of a submersible motor powered by photovoltaic cells is discussed. The designed motor consists of a semi-modular dual-stack. In a dual-stack rotor, a semi-modular rotor means one rotor module is kept fixed at one end and the other rotor module is kept floating in the other end. The dual-stack stator helps in increasing the flux density and decreasing the current density to obtain the constant torque outputs. For controlling the cogging torque development, the designed rotor magnets are skewed to a certain angle. Various parameters are to be considered while designing a submersible motor such as (i) selection of rotor magnet heights, (ii) selection of rotor outer radius, (iii) selection of the slot-pole combination. Submersible motor-driven using induction motor makes the system rugged and efficiency is less. Hence, submersible motor-driven using a brushless direct current motor is preferred for reducing the torque ripple of the BLDC motor.

D. DRONE

The Drone (unmanned aerial vehicles) operation characteristics are suitable for BLDC motor type single rotor and multirotor models as shown in Fig. 13 and Fig. 14. The flight of drones may operate manually, auto-pilot assistance, and autonomous aircraft. These drones need thrust to flow in the air. Hence, we use electric motors for developing thrust in the air, especially BLDC motors are used. Mostly IE-2 standard micropower BLDC motors are preferred for drone application. The main challenge in drones is to maintain constant torque in the BLDC motor to maintain high thrust at the base and fault tolerance capability for improving continuity in operations. In [67] BLDC motor behavior is analyzed in a time-domain function drone. A signal based on chaos using the density of maxima algorithm is used to improve the performance of the drone instead of a fast Fourier transform. BLDC motor exhibited extremely good characteristics in the proposed algorithm of drones. For improving drone stability, the calculations are made simple. In [68] FOC-controlled motor drive for drone algorithm is discussed. And FOC-controlled drone provides less torque and flux ripple compared to scalar control techniques, when a Fourier transform function uses vector control technique the computation intricacy of the machine is reduced. And the response of the drone is too efficient and the drone runs for more hours. In [69] the drone characteristic is improvised by using a Halbach array-based BLDC motor and response
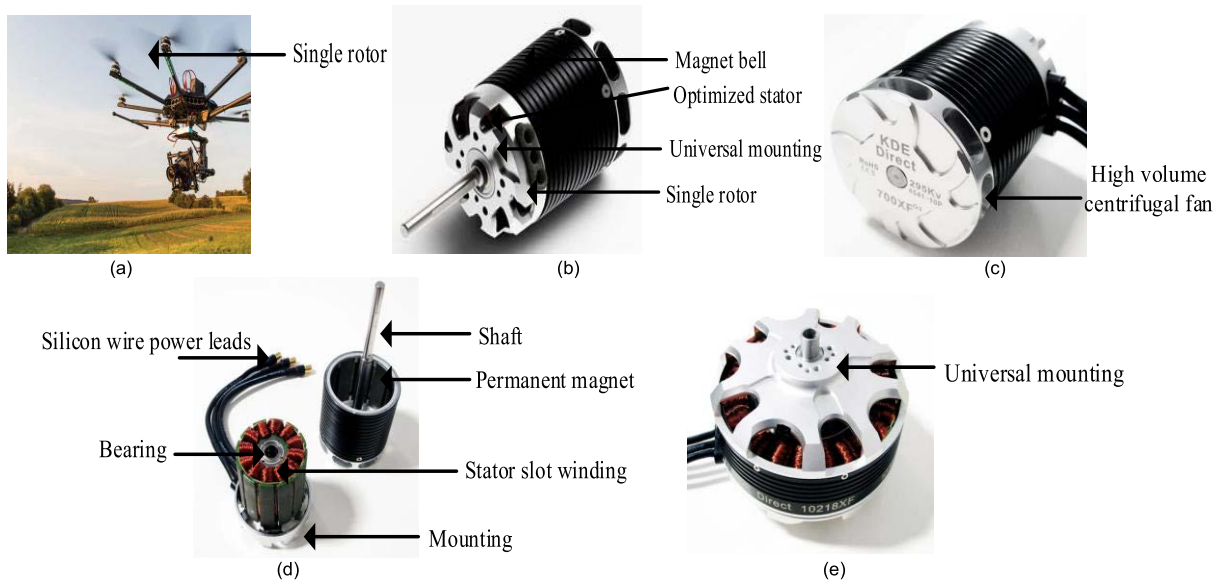
FIGURE 13. (a) Many Single rotors in a drone. (b) Single rotor motor model. (c) Volume size of motor. (d) Motor internal parts. (e) Motor mounting.
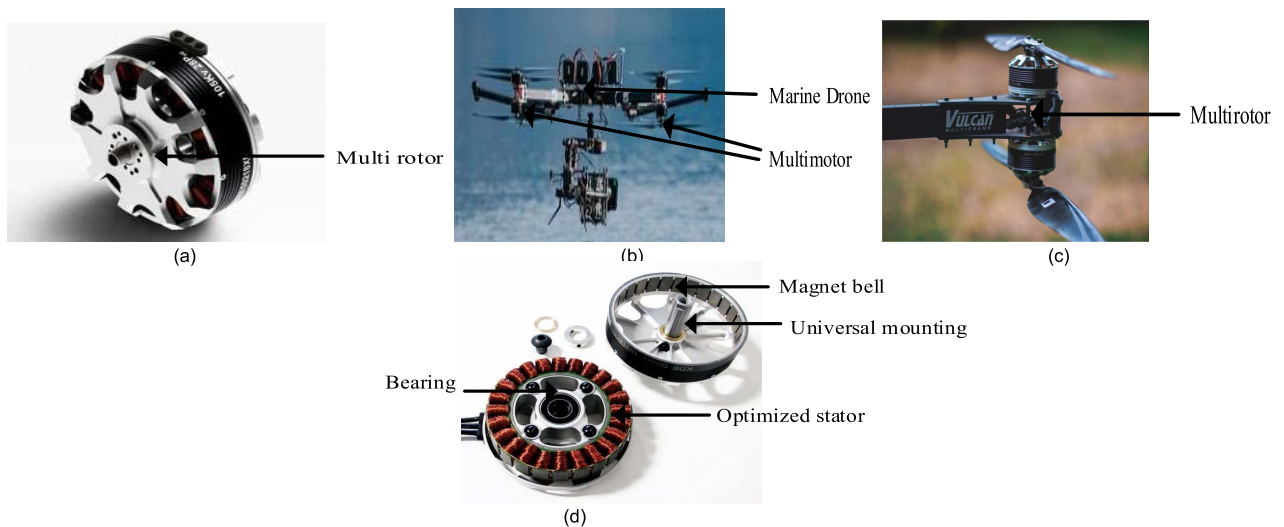

FIGURE 14. (a) Multirotor front view. (b) Multirotor drone model. (c) Multirotor view. (d) Multirotor internal part.

surface method. The Usage of Halbach array magnets and response face method reduces the losses of BLDC motors and improves the power characteristics.

E. INDUSTRY APPLICATIONS

In Industry, BLDC motors are preferred for various applications such as automation robots, hoists, elevators, conveyor belts, and CNC machines. Since BLDC motor has the advantage of providing fine torque in static applications without any ripples in torque compared to other motors these BLDC motors are preferred a lot. Inherent to the above advantages BLDC motor provides less inertia, high torque, and extensive operating speed.

The main challenges of BLDC motors in the industry are improving fault-tolerant capability, reducing EMI, and torque and flux ripple control. In this section, how the reliability

of BLDC motor is affected in industry and torque ripple effects are reviewed. In [70] a sensor less control algorithm for BLDC motor for reciprocating compressors is discussed. The peak current magnitude causes the demagnetization of permanent magnets in the rotor. These demagnetization currents are measured. The control algorithm is designed that commutation depends on the level of phase currents. The proposed technique improves the power and torque characteristics. In [71] scalar controlled BLDC motors for industrial applications are discussed. The realization of PWM signals in the motor controller is done with help of input and output ports in the microcontroller.

This simplifies the operation and improves the stability of the operation. In [72] torque developed in BLDC motors is reduced by model-based power control schemes. Active and reactive powers are used to control the torque of the
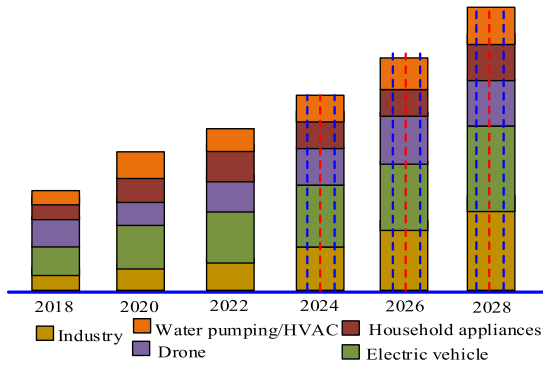
BLDC machine. Torque is controlled by seven voltage vectors and flux is controlled by two voltage vectors which help in efficient control.

F. HOUSEHOLD APPLIANCES

Traditionally single-phase induction motors were preferred for household applications which led to more energy consumption. Hence, it is necessary to develop a motor system with high energy efficiency and energy star requirement. Energy star deals with power reduction, robustness, and high performance. BLDC motors are used to save power in many household applications such as washing machines, water pumping, fan, air conditioner. These motors provide a good power factor as these motors run with help of a motor controller. In [73] inverter module is developed using silicon-controlled rectifiers. Using silicon-controlled rectifiers reduces the cost by 30 percent. In [74] space vector-based commutation is used for Fan application. Using SVPWM decreases the acoustic noise developed in the machine. In [75] a digital control-based BLDC motor drive is discussed. The main advantage of digital control is improving the response of the drive. The developed torque is also reduced.

Fig.15. depicts the end-user demand of BLDC motor on particular applications. From 2022 to 2028, it is analyzed that BLDC motors will be used mostly in consumer electronics, automotive, and industrial applications. Motors from 500-10000 RPM are preferred a lot. Inner rotor motors are mostly preferred to outer rotor motors. While reviewing the various applications of BLDC motors, the most challenging part is improving the fault-tolerant capability, reducing the torque ripples, and reducing the EMI. In the upcoming section, reliability control techniques and torque ripple mitigation techniques based on BLDC motor applications are reviewed.

IV. RELIABILITY CONTROL TECHNIQUES
A. FAULT-TOLERANCE CONTROL
Fault tolerance control (FTC) is a censorious process that is ultimately needed for complicated applications such as electrical vehicles, robotics, and certain dynamic applications.

The faults in a BLDC motor drive are classified into four types - (i) power switch open-circuit, (ii) power switch short circuit fault, (iii) DC-link capacitor short circuit fault, and (iv) hall-sensor failure. FTC can be classified into four techniques (1) replication FTC, (2) Failure oblivious computing FTC, (3) Recovery shepherding FTC, and (4) circuit breaker FTC. In BLDC motor drive systems replication FTC method is implemented. Replication FTC is considered with providing numerous instances of the system and switching it into one of the remaining instances in case of any failure in the system. For efficient fault-tolerant control, a model-based approach is mostly preferred. This model-based approach works on the principle of state estimation where the mathematical model of the system is predicted and the cost function (CF) estimation is performed. When the estimated cost function and threshold model are not similar. Fault code (FC) is generated. Thus, the FTC algorithm is performed. Fig. 16 represents the basic block diagram of fault tolerance control.

In BLDC, failure is considered with sensors out-performance in providing gate pulses. In [76] LRGF neural network scheme is implemented for fault diagnosis and detecting faults are also discussed. The neural algorithm is compared with the conventional motor drive algorithm, if any fault is detected the adaptive control system will manifest a certain signal as output. Using these signals, the incipient fault of the system is calculated using the incipient threshold and tolerance time. The neural network used in this system detects faults such as voltage leaks in drivers, mechanical and electrical faults of the system can also be detected. In [77] the failure of the hall-effect sensor in aerospace BLDC motors is analyzed. The analysis includes tests such as performance inspection, visual inspection, x-ray inspection. These tests are done to check the corrosion content in the corresponding sensor. The validation of the hall sensors after the corrosion is also discussed.

The ultimate need for fault tolerance diagnosis is also shown in [77]. In [78] a direct redundant FTC for the three-phase brushless direct current motor is discussed. The various instant at which gate pulses are generated are shown and these instants are compared with the generation of gate pulse generation with fault. Direct redundant control is achieved by using two hall sensor modules parallelly. The algorithm is designed in such a way that when one hall sensor is faulted. The output generated from other hall sensor modules is automatically chosen. The method of producing fault in gate pulse generation is also discussed. In [79] a method is used to detect the stator inter-turn fault in the BLDC motor. With help of stator inter currents during normal conditions is compared with the stator inter currents during fault conditions, the difference is converted as the energy spend. This parameter is compared with a threshold for fault detection. Since this process should be expeditious wavelet speed controller is used. In [80] simultaneous faults are taken into account. Simultaneous faults are classified into four types and hall sensor faults are classified into six types to attain fast FTC
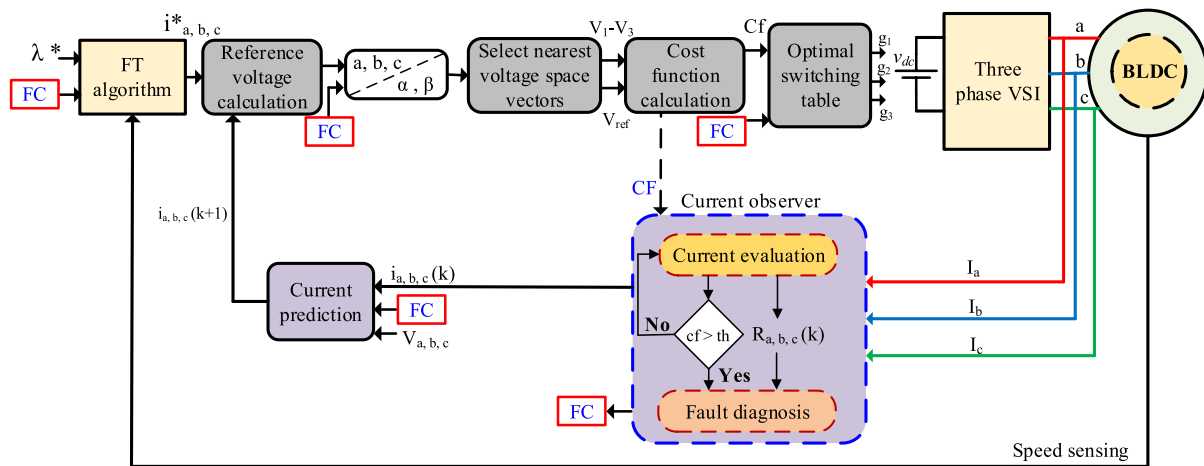
FIGURE 16. Fault-tolerant control technique.

TABLE 8. Fault diagnosis technology comparative analysis.

BLDC motor drive fault types	FTC topologies	Adopted techniques	FTC ideology	Ref
Power converter fault	• Model predictive control • Direct torque control • Field oriented control	• FTC control is attained by increasing the dc-link bias voltage and reducing torque ripple	• Bidirectional converters, motor drive systems with fast fusing capability are used	[76], [83,84]
Permanent Magnet demagnetization fault	• Predictive control method • Observer method	• By maintaining less flux ripple and torque ripple	• Optimizing rotor magnetic materials and magnetic circuits	[85]
Sensor fault 1. Current sensor 2. Voltage sensor 3. Speed sensor	• Observer method • Impedance salient pole • Fundamental wave model • DC bus sampling method	• Algorithms used to re-evaluate the speed and current under normal condition	• Speed sensor redundancy methods and fault code diagnosis are used	[77,78]
Stator winding fault	• Minimum torque ripple principle • Invariance MMF principle	• Torque ripples are minimized using feed-forward compensation and decoupling transformation principle	• The star-point of the motor is connected to the dc bus of the drive system and multiphase motors are used	[79]

the time transition for each hall sensor is calculated accurately and the degree of rotation is also taken into account. When a mismatch is encountered between threshold time and real-time signal generation, reconstructed signals are generated automatically. In [81] FTC for multiphase motors is discussed. The main purpose of using multiphase motors is to achieve high torque and power density. FTC is achieved by controlling the faulty phase currents with the healthy phase currents. In [82] the FTC is achieved by an additional phase leg and fault protective circuits. When there is the detection of open-circuit faults in both buck converter and inverter region, FTC is achieved by choosing the redundant switch present in between inverter and motor. In [84] FTC three-phase BLDC motor is discussed. FTC is achieved by using a modular architecture where three individual control loops which regulate the phase current for each phase gate pulse. The errors are regulated by PI controllers. In [85] a BLDC motor drive system that has less electromagnetic interference

and FTC is discussed. The EMI is controlled by using stray capacitance between cables and the ground plate. FTC is achieved by ten legs and five modules topology. The FTC capability is investigated using the meantime failure analysis. The various fault and techniques are compared in Table 8.

B. ELECTROMAGNETIC INTERFERENCE CONTROL

Electro-Magnetic Interference (EMI) is defined as electromagnetic signals which interfere with electrical equipment such as motor, variable frequency drives, power converters, etc., EMI is an undesirable disturbance to an electric circuit. EMI affects machine performance, efficiency, etc., EMI can be classified into (i) radiated EMI and (ii) conductive EMI. Fig. 17. represents the basic block diagram of the electromagnetic interference algorithm [86]. Conductive EMI is the electromagnetic interference between the source and victim which is caused through conductors and Radiative EMI is
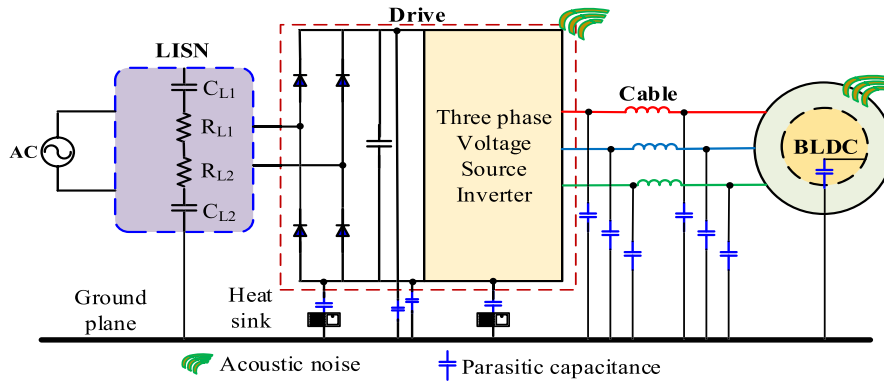
FIGURE 17. Electromagnetic interference control.

the electromagnetic interference between the source and then victim caused through a wireless medium [87].

Conducted EMI is found to occur at lower frequencies. It is further classified as differential mode and common mode. Common mode EMI source is found to be at high source and low impedance. Differential mode EMI is caused by pulsating currents.

Techniques used to mitigate EMI are classified as follows:

1. EMI filter and shielding
2. Random modulation
3. Chaotic PWM

1) EMI FILTERS AND SHIELDING

EMI filters are used to reduce the interference in transmission lines and power cables. EMI filters provide high input resistance to control the frequency content. The main objective of the EMI filter reduces the interference between other electronic devices. EMI filters are further classified as (i) Active filters, (ii) Passive filters, and (iii) Hybrid filters. LISN is used to stabilize the impedance present in the circuit and pure power without EMI content.

In [88] an organized EMI filter was designed to separate the unwanted noise in a three-phase inverter. The noise level was reduced to 40dB μV. In [89] Angle modulated switching strategy is used to control the EMI in a BLDC motor drive. The advantage of using this scheme to reduce the EMI filter size to 50% and the noise level is suppressed to 10dB μV. In [90] passive filters are designed to control the EMI generated by the machine. The inductor and capacitor are connected parallel and controls the dv/dt and di/dt spikes in the circuit. The stages of LC are increased depending upon the dv/dt and di/dt changes.

2) RANDOM MODULATION

In random modulation, the switching frequency is varied depending upon the given random signals. Whenever optimal switching frequency is given to the power switch. The unwanted power losses generated are reduced. The disadvantages of this technique are (i) computing random

signals makes the control algorithm complex (ii) the parameter designing complexity increases. In [93] to reduce the EMI content wait-free phase continuous carrier frequency modulation technique is used. WPCFM and digital synthesizer theory is combined to obtain a fast response and effective EMI control. In [91] spectrum modulation technique is used to control the EMI content. The spectrum modulation techniques reduce the EMI to 5-10dB.

3) CHAOTIC PWM

The pulses for various power switches in the inverter are developed using various PWM techniques. This technique not only reduces the torque ripple of the machine, but it also owes to reducing various losses and improving the reliability of the converter. The development of EMI is also reduced. In [92] complementary PWM technique is used to mitigate the electromagnetic emissions in a three-phase inverter. The common-mode emissions are controlled by the bipolar PWM technique. Thus, owing to a reduction in EMI. The various EMI techniques and their suppression levels are compared in Table 9.

C. ACOUSTIC NOISE CONTROL

Acoustic noise control for motor drive systems is one of the most researched topics by scholars [96]. Only a few papers are discussed for BLDC motors. Acoustic noise is caused due to many reasons. The major reasons are (i) Torque ripple generation (ii) electromagnetic fluctuation (iii) non-ideal spatial distribution of flux density between rotor permanent magnet and the stator slot openings (iv) generation of the harmonic component due to non-ideal distortion of radial flux. The intricacy in the algorithm increases with controlling electromagnetic fluctuation and torque ripple of the BLDC machine. These acoustic noises and vibrations affect increasing EMI content and bearing current generation. The generation of bearing is one of the most important topics which many researchers focus to mitigate. Bearing current generation leads to motor bearing lock [97].

TABLE 9. Comparison of EMI Control technique and its suppression level.

EMI Topology	Type of converters	Switching frequency	Suppression level	Ref
Chaotic PWM	• Three phase VSD using multi-carrier PWM algorithm	3KHz	30% improvement than conventional	[86]
EMI filter	• Three Phase inverter fed to the motor controller	15 KHz	40dB	[88]
Angle modulated switching strategy with EMI filter	• Single phase fractional power BLDC motor drive	20 KHz	10dB	[89]
Bipolar PWM	• Three phase BLDC motor drive.	10 KHz	20% improvement than conventional	[92]
CFMPWM and CAPWM	• Three phase motor drive	150 KHz	4.6dB and 5.6dB	[95]
AC and DC side EMI filter	• Three phase motor drive system	2-5 MHz	40dB	[94]
WPCFM	• Three phase PMSM motor drive	10-20KHz	10dB	[93]
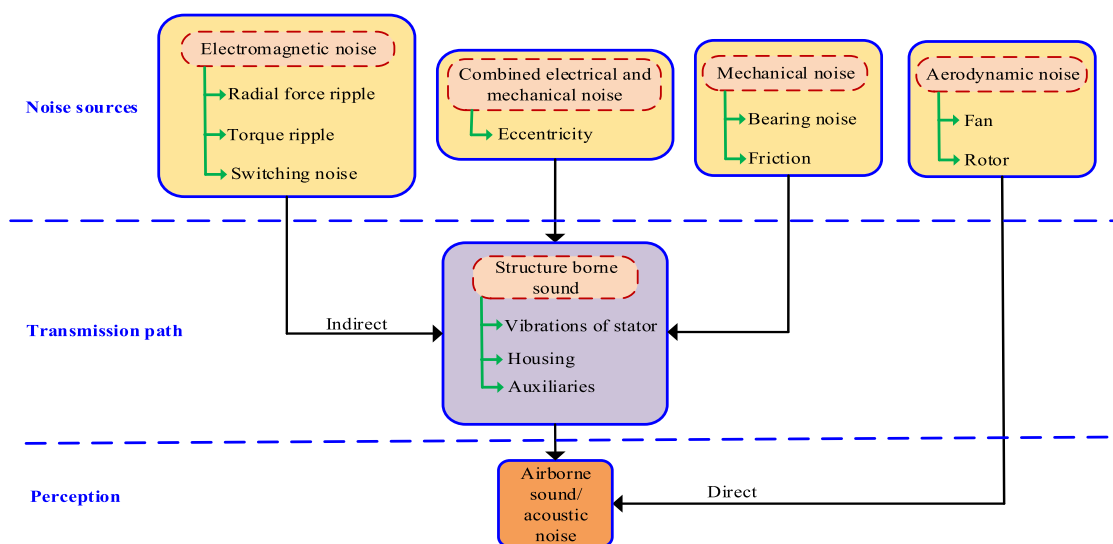
FIGURE 18. Source of acoustic noise.

The acoustic noise generation depends on various sources such as mechanical noise, noises developed due to efficient designing, electromagnetic fluctuation, poor alignment, and aerodynamics of the machine. Fig. 18 depicts the various sources of acoustic noises and the transmission path of the system.

One of the most difficult operations in acoustic noise control is analyzing the root cause of the issue and measuring the amount of noise generated [98]. The amount of noise generated is measured using a microphone and accelerometer integrated with embedded controllers Fig. 19 depicts the block diagram of the methodology used to analyze the acoustic noise issue.

Many researchers have discussed several topologies to reduce acoustic noise for BLDC motors both in design and motor-drive system control algorithm topology. In [99] the field distribution in between the air gap region of the

permanent magnet is measured instantaneously on various load conditions and analyzed various remedy actions to reduce the acoustic noise developed. The effective method was found to be using slotted stator slots and an embedded permanent magnet rotor. In [100] optimized pole magnetic strategy is used to control the field harmonics and analyzed the origin of the acoustic noise issue. In [101] the torque and flux ripples are predicted as stator currents. In sinusoidal commutated BLDC motors, due to field weakening radial forces developed are reduced. To optimize this issue, a moving band technique with special quadrilateral elements is used.

During the analysis, it was found that the developed technique reduces acoustic noises by 30%. In [102] the third harmonic component in air gap flux density is eliminated. The third harmonic component is managed by forming optical notches in the rotor. Using notches in the rotor reduces the air
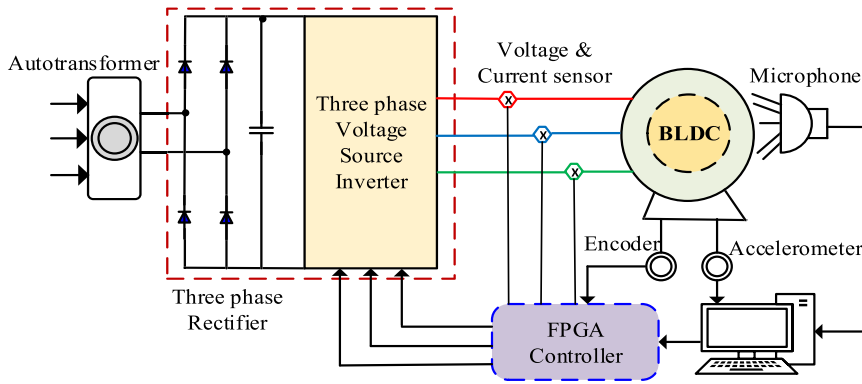
FIGURE 19. Acoustic noise control.

gap in the BLDC motor which helps in reducing the acoustic noise developed by the motor. In [103] the acoustic noise developed is reduced by using a voltage regulation circuit for a single-phase BLDC machine which is used for fan application. Fans generate more noise due to their aerodynamic design and the humming noise also increases with variation in speeds. The designed voltage regulator consists of an inductor connected parallel to the series resistance and the capacitor element. The developed technique reduced 16.1% of developed acoustic noises compared to conventional techniques.

In [104] the acoustic noise development is analyzed by using a novel digital PWM technique. The digital PWM is developed for a scalar-controlled BLDC motor drive system. The odd-order harmonics are reduced. The developed technique reduces the noise content to 15-30dB. In [105] a sinusoidal BLDC machine is designed to control the acoustic noises in machine. Using this method, the electromagnetic fluctuation is controlled. While analyzing various acoustic noise control techniques, it found that on loaded condition increase in toque ripple improves the acoustic noise generation six times. Reduced torque ripple and flux ripple reduce the acoustic noise generated in BLDC machines.

V. TORQUE RIPPLE MITIGATION
A. SOURCES OF TORQUE RIPPLE
Torque ripples are developed due to several reasons [106]. Various sources for the development of torque ripple are discussed below and shown in Fig. 22.

1) STRUCTURE OF MOTOR
The structure of the motor depends on various factors such as power, speed, loading perspective, etc., these structure-based factors are constrained with reasons such as airgap, flux linkage, non-sinusoidal back-EMF.

2) NATURE OF MOTOR
The motor nature depends on the various materials that we have used during the construction process. Hence, picking the correct material is very important. The main factors are Cogging torque, Reluctance torque, Electromagnetic torque.
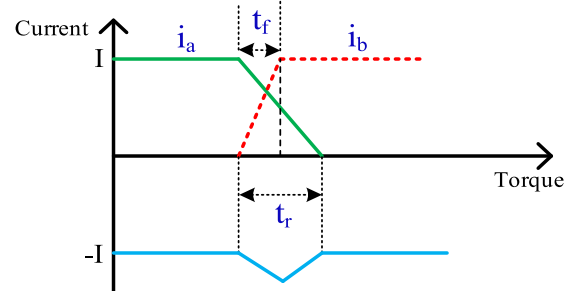

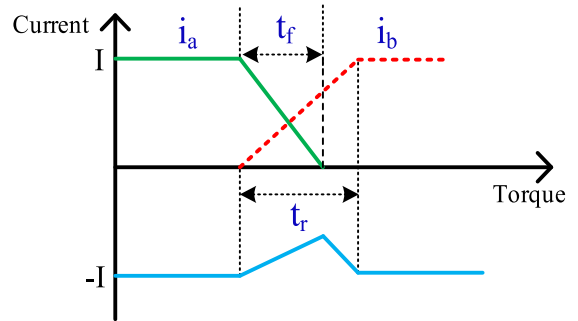**FIGURE 20.** Phase current and Back EMF waveforms.

FIGURE 21. Phase current and Back EMF waveforms.

3) CONTROL OF MOTOR
Torque ripples are developed from motor control through inefficient commutation strategies and internal gate control schemes.

Ideally, the torque ripple is constant due to the in-phase back EMF and quasi square wave stator current. But practically this is not possible due to the nonzero inductance of the stator winding which leads to the development of torque ripple. The following graphs represent the effect of phase currents on torque waveforms.

Fig. 20 shows that the incoming current in phase B reaches a steady-state before current phase A reaches zero. Torque ripple is due to the commutation of motor current. t_r and t_f are the rise time and fall time respectively.

The outgoing current in phase A becomes zero before the current in phase B reaches a steady state as shown in Fig. 21. Torque dip is due to the commutation of motor current.
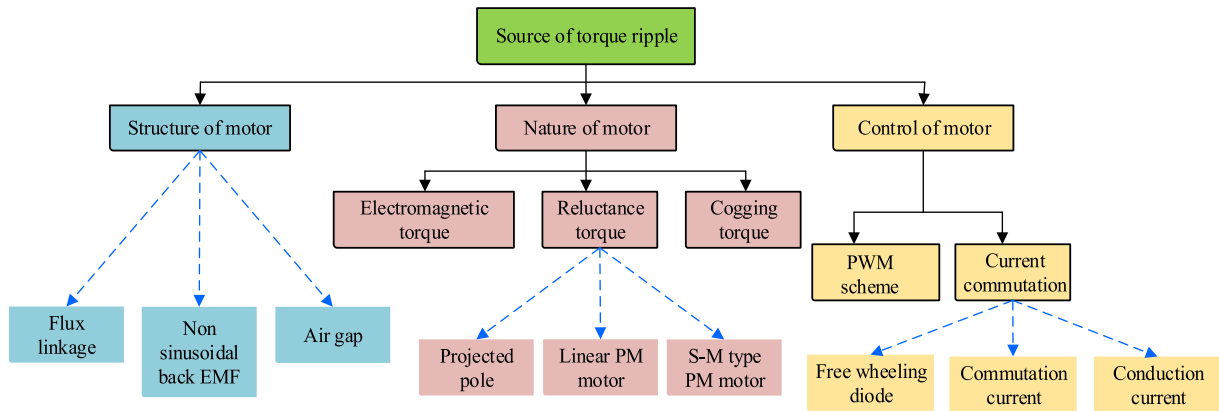
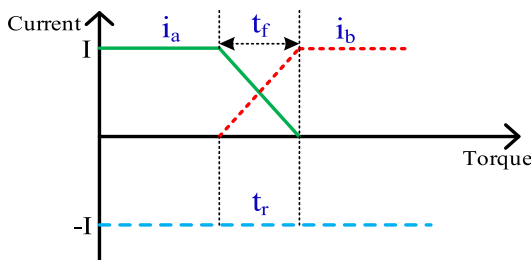**FIGURE 22. Sources of torque ripple in BLDC motor.**

FIGURE 23. Phase current and back EMF waveforms.

The slope of outgoing current in phase A becomes equal to the slope of incoming current in phase B. At this commutation, instant torque remains constant and is represented in Fig. 23.

a: TECHNIQUES OF TORQUE RIPPLE MITIGATION
In recent years many types of research have been done in torque ripple mitigation in BLDC motors which mainly include (i) Field orientation control technique, (ii) Direct torque control technique, (iii) Current shaping techniques, (iv) Controlling input voltage, (v) Intelligent control, and (vi) Drive-inverter topology

B. FIELD ORIENTATION CONTROL TECHNIQUE
One of the ancient techniques for torque ripple mitigation is FOC. Fig. 24 depicts the block diagram of the FOC control algorithm of the BLDC motor. In a permanent magnet motor, the desirable output is obtained when the rotor and stator flux linkages are 90°.

In FOC, the feedbacks are obtained as voltage and current vectors. The development of space vector pulse width modulation schemes led many researchers in the development of the latest inventions in FOC. The stator currents are mostly characterized as (1) Torque and (2) Flux. In [106] the difficulties of inserting rotor at correct angles in a permanent magnet motor is discussed elaborately. For the

implementation of such a system, the researcher has used a digital signal controller using a microcontroller (STM32F407). In this technique the rotor positions are obtained by implementing the encoders, after inserting the rotor, the encoder pre-set details are reset, and then for high hold on torque, the duty cycles of PWM signals are increased. Thus, the step bugging operation is achieved. In [107], a comparative study of FOC schemes and DTC schemes for five-phase permanent magnet motor is discussed. Five phase permanent magnet motors are in use as they have reduced torque harmonic content compared to three-phase permanent magnet motors. The stator flux orientation control is implemented by obtaining the relative position d-axis and q-axis of stator and rotor teeth. The development of the *dq*-axis in the stator is very important for implementing vector control.

In [108], FOC control for a BLDC machine is discussed. Cogging torque profile is suitably included in q-axis current reference, which must be then precisely tracked to mitigate torque ripple and speed ripple caused by cogging torque.

This technique is also used to mitigate acoustic noise and vibration. Therefore, the dynamic equations are obtained using two-pole electrical machines, and then these equations are converted to two-coordinate system by realizing them with a reference locking with d-axis waveforms. In [109], the FOC control system for the BLDC motor is discussed. FOC control technique to drive BLDC motor-based compensation torque ripple. By mismatching, the non-trapezoidal back EMF and stator current the torque fluctuation can be controlled by an active and reactive power control loop. Implemented two vector control finite control set model provides good steady-state and fast torque response.

C. DIRECT TORQUE CONTROL TECHNIQUE
In the direct torque control technique, the variables relating to the flux linkage and torque are used to select the voltage vectors. These details are processed and the errors are obtained. These errors with further reference signals are processed in a hysteresis controller. Using DTC, the torque is controlled by controlling the flux of the system. DTC technique is
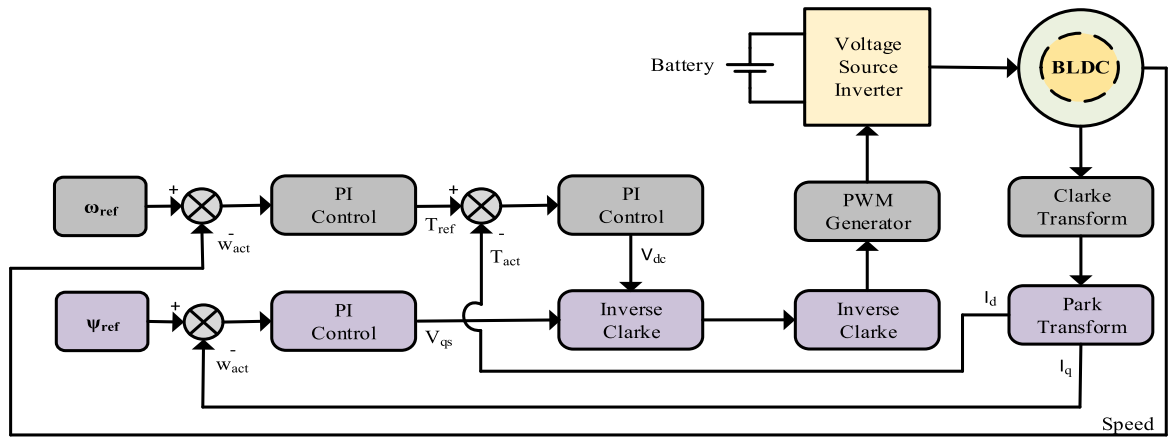
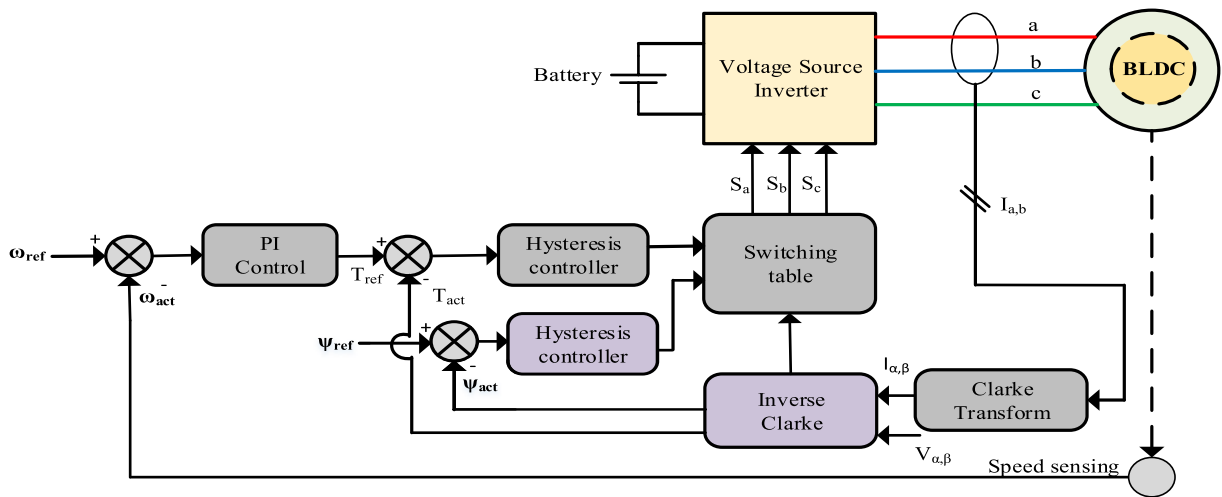**FIGURE 24.** Field orientation control of BLDC motor.

FIGURE 25. Direct torque control of BLDC motor.

mostly preferred as it can verify its control schemes and is easier to operate. Fig. 25. depicts the block diagram of the DTC technique of the BLDC motor. In [110], [111], a DTC scheme with an active null vector control strategy is discussed elaborately. In the proposed strategy the signs of error are determined by the two-level flux and torque hysteresis comparator. Here the torque slopes, the switching time is calculated with the above inputs, and the torque of the motor can be estimated. This scheme has the advantage of comparing torque and flux responses of various vectors.

Twelve-step direct torque control is introduced to control the vectors with help of a five-level hysteresis controller. In the proposed scheme the vectors are divided into twelve sectors which means for every thirty degrees of rotation, the current and voltage parameter is uploaded to the controller [112]. It has been discussed clearly that torque ripples can be mitigated by maintaining constant current and varying the frequency from low to high by using the DTC technique. Stator fluxes are controlled by using hysteresis controllers. In [113], the Torque ripple of the induction motor

is reduced by integrating the CSFTC-DTC scheme with a neutral point clamped multilevel inverter. The CSFTC maintains the switching frequency constant. However, the proposed technique reduces the output torque but the strategy used for controlling is very complex.

D. CURRENT SHAPING TECHNIQUE

The current shaping technique refers to dodging the gate pulse generation in power switches of VSI when an abnormal event such as overcurrent, speed up, and overloading is detected. Fig. 26. depicts the block diagram of the current shaping technique of the BLDC motor. Generally, the steps followed by this scheme are sensing high current, recognizing overcurrent events, turning off logic, and re-enabling action for high current detection. In [114], a technique where the torque ripples are reduced by using the small capacitors is discussed. The charging and discharging of the capacitor may return high voltage to the input system which might damage the drive system. A new turn-off logic scheme is introduced which would not affect the power switches.
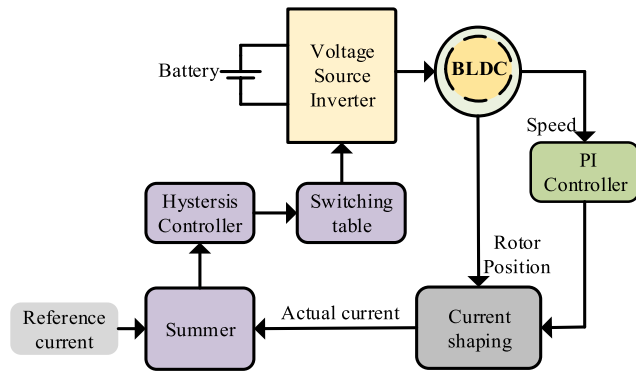
FIGURE 26. Current shaping technique of BLDC motor.

Changing the turn-off logic means keeping one switch down during the current limit. In [115], current hysteresis control to control the BLDC motor current directly is discussed in detail. In addition, a novel transition control method is also discussed. The non-commutation phase should be constant during commutation interval for proper current hysteresis control. The outgoing phase current should reduce as quickly as possible. The sum of the absolute value of the incoming phase and outgoing phase current should be constant.

By implementing this technique, the switching losses can be reduced. In [116], torque ripple mitigation using one cycle control is discussed in detail. This technique explains a new topology where back EMF and rotor position information is neglected. One cycle control means each switch is operating for one-third of the fundamental cycle which means it is turned on for sixty electrical degrees and operating in PWM for the next sixty electrical degrees. Even order harmonics are also reduced using this scheme. In [117], torque ripple is reduced by finding the correct commutation point by

auto-calibrating the phase shift. The dc bus details are obtained for processing these details to the controller.

E. CONTROLLING INPUT VOLTAGE

BLDC motors are used in several applications as they have high torque to speed ratio, high efficiency, fast dynamic response, lesser maintenance, etc., Fig. 27 depicts the control diagram of input voltage controlling technique of torque ripple mitigation of BLDC motor. The special features are trapezoidal back EMF and quasi square wave fed phase current. Torque ripples are generated when there is in-equivalency predicted between back EMF and quasi square wave fed phase current. In this phase, we are going to investigate a technique for controlling torque ripple by controlling the input voltage. This scheme for controlling the input voltage has been investigated by several researchers. Controlling ways of the input voltage can be categorized as PWM schemes and varying dc-link voltage. Usually, torque ripple is caused by the commutation of power switches. This commutation can be controlled using the PWM scheme. In [118], a neoteric method for reducing torque ripple during both conduction and commutation through a closed-loop operation using a PWM scheme with buck converter is discussed elaborately. The PWM schemes are categorized into two steps, firstly controlling the commutation using PWM schemes and secondly by using buck converter which converts v_{in} to v_{out}.

In [119], a novel PWM scheme using a bootstrap circuit is discussed. The conventional six-step inverter is integrated with a bootstrap circuit and a new PWM driving scheme is introduced. The theoretical results are convincing with the performance. In [120], the various PWM schemes are analyzed. Compared to conventional PWM schemes, digital PWM is economic and more effective proved by experimental results. In [121], a method for reducing torque ripple is investigated using the technique of varying input voltage. In this technique, the diode of the upcoming phase power switch
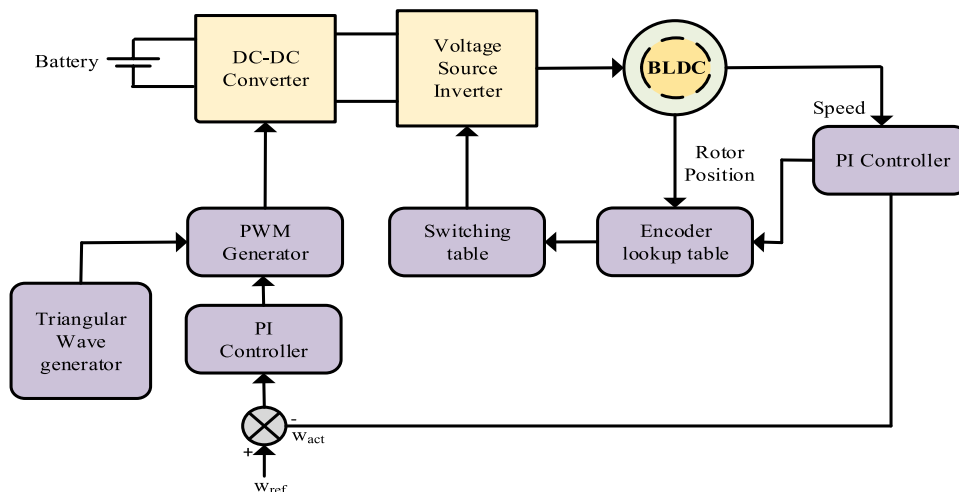

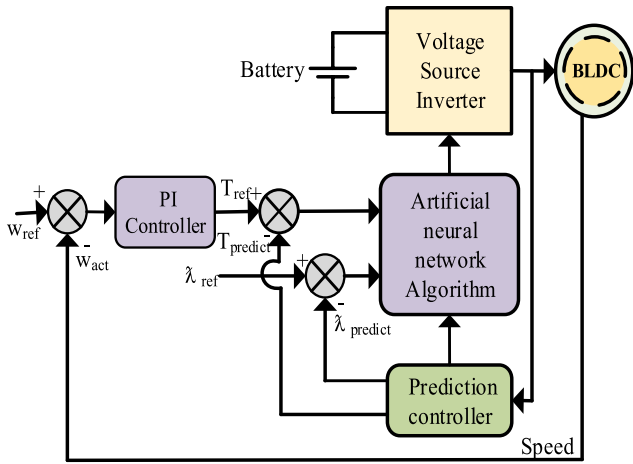
FIGURE 27. Controlling input voltage of BLDC motor.

FIGURE 28. Intelligent controller of BLDC motor.

FIGURE 29. Drive inverter topological control of BLDC motor.

will switch on during the commutation of the outgoing phase switch. This may improve the speed of ripples. To reduce it, the outgoing phase switch is kept on even after the phase outgoes. In [122], converter topology for both modified single end primary inductance converter and three-level neutral point clamped multilevel inverter is integrated and investigated in detail. These integrated topologies give good results compared to the previously discussed topologies.

F. INTELLIGENT CONTROL

Controlling torque and flux without a controller is impossible. Hence, a controller is necessary for every mitigation technique Compared to the other techniques, implementing an advanced controller has the advantage of analyzing several parameters. Conventional PI and PID controllers are used in industries and several applications. Fig. 28. depicts the block diagram of intelligent control technique of torque ripple mitigation of BLDC motor. In [124], a fuzzy logic estimator is investigated to reduce the torque ripples.

The function of this neural scheme concept-based controller is to regulate the commutation angle to maintain the slew rates of the commutated phase while keeping the non-commutating phase current constant. In this scheme, both the motor winding parameters and output parameters such as torque are analyzed and a new commutation is generated. In [125], an integrated loss minimization control and a wavelet speed controller performance are discussed in detail. The speed errors between actual and command speeds are given as input to the loss minimization controller. These outputs are processed using power processing units which helps us to reduce the torque ripples of the drive output. In [126], a spider web-based algorithm integrated with a small capacitor for varying dc-link voltage is discussed in detail.

The algorithm and feedback are compiled and used to generate the switching sequences. In [127], the torque ripple of the BLDC motor is reduced by using a model predictive control algorithm the learning is done for varying speed and
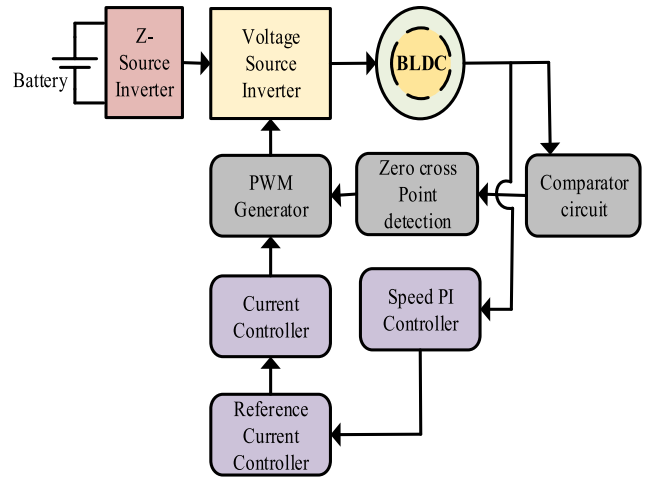
the gate pulse generating algorithm of the conventional system. Using this strategy, a new method is observed and gate pulse is generated. The output of the concerned technique contains fewer torque ripples.

G. DRIVE INVERTER TOPOLOGY

Z-source inverters (ZSI) are single-stage power converters with voltage buck-boost capabilities. The z-source is placed in between the voltage source and inverter to boost the voltage from the voltage source. The advancement in this feature led to the development of quasi-Z-source, switched inductor z-source, etc., Fig. 29. Depicts the block diagram of drive inverter topology operated motor controller of BLDC motor. In [128], a drive system integrated with quasi-Z-source is discussed in detail. Since quasi-Z-source is meant for increasing the source voltage, a shutdown network is installed in-between z-source and voltage source for controlling the output voltages. A new control system for space vector modulation is also discussed. The torque ripple mitigation is achieved by a hybrid topology of two processes predictive control and voltage-based torque ripple mitigation. The results are evidence that this technique has more advantages than the conventional technique constant dc source. [129] discusses the model and design of a permanent magnet brushless dc motor which is fed by a Z source inverter. The paper discusses the limitations of permanent magnet BLDC motor (PMBDCM) and explains about two techniques to overcome the limitations of PMBDCM powered by fuel cell, of which one technique is using Z-source inverter. The paper discusses the advantages of Z source fed PMBDCM like higher efficiency, bucked/boosted voltage ability, and feasibility of adjustable speed drive systems with motors like PMBDCM.

The ZSI is coupled with PWM to get 120° square waveforms which are said to be apt for the system.

Various state-space models such as the impedance source network and voltage source fed permanent magnet brushless

TABLE 10. Comparison of various torque ripple mitigation techniques of BLDC motors.

Methods	Adopted Technique	Advantages	Disadvantages	Reference
Field orientation control	Analysis of the d-axis and q-axis is done and these parameters are fed to the controller for optimization.	Sinusoidal phase current, low torque ripples, torque control at a lower speed.	Rotor sensors need to be used for induction motors, FOC sensors are less reliable.	[106-109]
Direct torque control	The variables relating the flux and torque are used to select the voltage vectors. These details are processed using the controller to the drive system for analysing the commutation point.	Fast dynamic response at high speeds, torque, and stator flux decouples, verifying the effectiveness of control schemes.	Complex calculations are needed, the poor dynamic response at slow speed.	[110-113]
Current shaping technique	Changing the switching logic whenever over current, speed up, and overloading is detected.	Reduced torque ripple, fast response, reduced voltage ripple.	Complicated and Difficult to understand.	[114-117]
Controlling input voltage	Regulating the PWM schemes by enhancing the control systems and regulating the dc-bus voltages by using DC-DC choppers.	Reduced torque ripple, possibilities of implementing hybrid topologies.	Costly, the response at a slow speed is very bad.	[118-122]
Intelligent controller	Used for analyzing several parameters from the motor by main techniques involving artificial neural network algorithm.	Reduced harmonic content, strong self-learning, and adaptive ability.	Complex computational algorithms.	[124-127]
Drive Inverter topology	Uses multilevel inverters and modified z-source topologies.	Torque ripple reduces, common-mode voltage reduces, and implementing hybrid topologies is possible.	Costly, separate protection is needed for power switches.	[128-131]
Sliding mode control	Sliding mode control theory is used to design a controller.	Anti-interference maximum ability is high. Robustness is less affected by parameters.	Difficult control to design, existential chatting, and high computing power are required	[132]
Model adaptive control	An offline model-based control is used for speed control resulting in the reduction of torque ripples.	The gain of the filter is adapted to reduce torque ripple.	The high sampling rate, Maximum precision requires high computing power, increasing the cost of digital controllers.	[133]
Modified PWM control	PWM chopping method. Low-cost digital control technique.	Higher output torque lower ripples, minimum cost, motor control hardware is complex.	Eliminating only torque ripple caused by stator magnetic field.	[134,135]

dc motor are compared and the equivalent circuit of both the systems are shown to bring in a comparative difference between the two systems. The simulation waveforms are also depicted which show that the system works like a VSI fed permanent magnet BLDC motor. After the first second when the necessary boosted function is fed to the system, it displays shoot through intervals, and the capacitor voltage is boosted up to 400V. Along with this, the torque and rotor speed also increases to their rated values. Two boost control methods for a Z source inverter are shown in [130].

The paper discusses the flaws of a normal voltage source inverter whose maximum boosted voltage cannot exceed the DC bus voltage. The system shows the design of boost control which gives maximum output value for any modulation index. To reduce the cost of the boost control, there should be a constant shoot-through duty cycle or duty ratio which is shown in this paper for five different modulation curves. A comparison of several control methods is conducted and it is concluded that the maximum boost control for the ZSI eliminated low-frequency ripples in the output frequency and

voltage stresses were also minimized. In [131] discusses the control methods of ZSI and compares voltage boost and modulation index. The paper initially discusses the PWM technique used in a 3 phase VSI whose gating sequence for voltage boost can be applied to ZSI with a few modifications in the shoot through. A few equations of voltage boost and voltage stress are shown and depicted and the comparisons are put forward using the equations. The simulation of maximum boost control shows that the voltage gain is the same for the same modulation index and increase modulation index. The paper shows the two control methods used for extracting the maximum boosted voltage of the ZSI and also shows a clear study on the relationship between boosted voltage and modulation index.

VI. CONTROL TECHNIQUES EQUATIONS AND COMPARISON

The comparison of various torque ripple mitigation techniques of the BLDC motor is illustrated in Table 10. The above-mentioned topologies are mentioned and compared
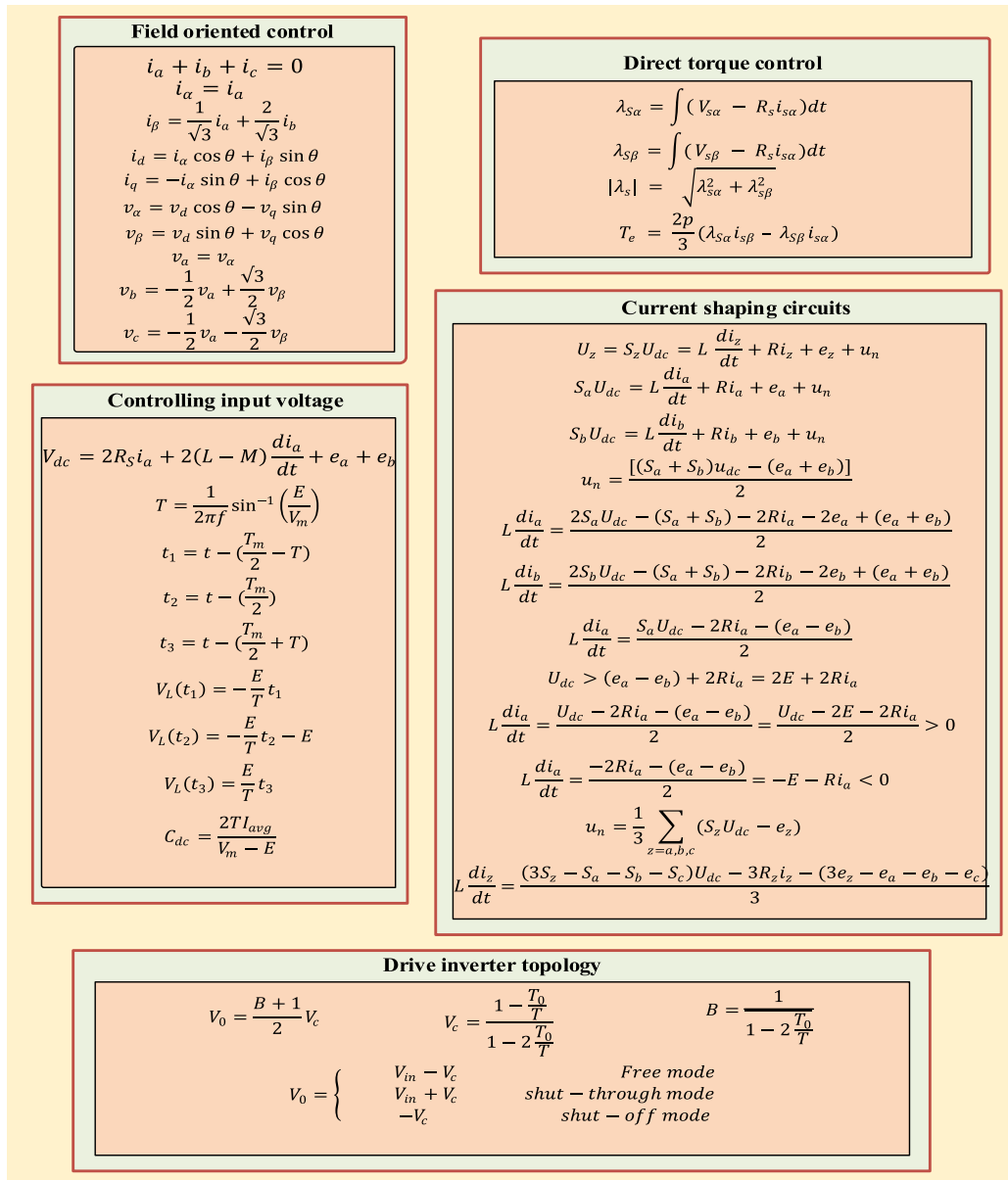
Field oriented control

$$i_a + i_b + i_c = 0$$
$$i_\alpha = i_a$$
$$i_\beta = \frac{1}{\sqrt{3}} i_a + \frac{2}{\sqrt{3}} i_b$$
$$i_d = i_\alpha \cos\theta + i_\beta \sin\theta$$
$$i_q = -i_\alpha \sin\theta + i_\beta \cos\theta$$
$$v_\alpha = v_d \cos\theta - v_q \sin\theta$$
$$v_\beta = v_d \sin\theta + v_q \cos\theta$$
$$v_a = v_\alpha$$
$$v_b = -\frac{1}{2} v_\alpha + \frac{\sqrt{3}}{2} v_\beta$$
$$v_c = -\frac{1}{2} v_\alpha - \frac{\sqrt{3}}{2} v_\beta$$

Direct torque control

$$\lambda_{S\alpha} = \int (V_{s\alpha} - R_s i_{s\alpha}) dt$$
$$\lambda_{S\beta} = \int (V_{s\beta} - R_s i_{s\alpha}) dt$$
$$|\lambda_s| = \sqrt{\lambda_{s\alpha}^2 + \lambda_{s\beta}^2}$$
$$T_e = \frac{2p}{3} (\lambda_{S\alpha} i_{s\beta} - \lambda_{S\beta} i_{s\alpha})$$

Controlling input voltage

$$V_{dc} = 2R_S i_a + 2(L - M)\frac{di_a}{dt} + e_a + e_b$$
$$T = \frac{1}{2\pi f} \sin^{-1}\left(\frac{E}{V_m}\right)$$
$$t_1 = t - (\frac{T_m}{2} - T)$$
$$t_2 = t - (\frac{T_m}{2})$$
$$t_3 = t - (\frac{T_m}{2} + T)$$
$$V_L(t_1) = -\frac{E}{T} t_1$$
$$V_L(t_2) = -\frac{E}{T} t_2 - E$$
$$V_L(t_3) = \frac{E}{T} t_3$$
$$C_{dc} = \frac{2T I_{avg}}{V_m - E}$$

Current shaping circuits

$$U_z = S_z U_{dc} = L\frac{di_z}{dt} + R i_z + e_z + u_n$$
$$S_a U_{dc} = L\frac{di_a}{dt} + R i_a + e_a + u_n$$
$$S_b U_{dc} = L\frac{di_b}{dt} + R i_b + e_b + u_n$$
$$u_n = \frac{[(S_a + S_b)u_{dc} - (e_a + e_b)]}{2}$$
$$L\frac{di_a}{dt} = \frac{2S_a U_{dc} - (S_a + S_b) - 2R i_a - 2e_a + (e_a + e_b)}{2}$$
$$L\frac{di_b}{dt} = \frac{2S_b U_{dc} - (S_a + S_b) - 2R i_b - 2e_b + (e_a + e_b)}{2}$$
$$L\frac{di_a}{dt} = \frac{S_a U_{dc} - 2R i_a - (e_a - e_b)}{2}$$
$$U_{dc} > (e_a - e_b) + 2R i_a = 2E + 2R i_a$$
$$L\frac{di_a}{dt} = \frac{U_{dc} - 2R i_a - (e_a - e_b)}{2} = \frac{U_{dc} - 2E - 2R i_a}{2} > 0$$
$$L\frac{di_a}{dt} = \frac{-2R i_a - (e_a - e_b)}{2} = -E - R i_a < 0$$
$$u_n = \frac{1}{3} \sum_{z=a,b,c} (S_z U_{dc} - e_z)$$
$$L\frac{di_z}{dt} = \frac{(3S_z - S_a - S_b - S_c)U_{dc} - 3R_z i_z - (3e_z - e_a - e_b - e_c)}{3}$$

Drive inverter topology

$$V_0 = \frac{B+1}{2} V_c \qquad V_c = \frac{1 - \frac{T_0}{T}}{1 - 2\frac{T_0}{T}} \qquad B = \frac{1}{1 - 2\frac{T_0}{T}}$$

$$V_0 = \begin{cases} V_{in} - V_c & Free\ mode \\ V_{in} + V_c & shut-through\ mode \\ -V_c & shut-off\ mode \end{cases}$$

FIGURE 30. Control techniques mathematical equation.

in terms of the adopted technique, advantages, and disadvantages. The topological equations used to control various torque ripple mitigation techniques are depicted in Fig. 30.

In a comparison of various torque ripple mitigation techniques dealt with control schemes, it is inferred that controlling torque ripple at a wide speed range is too difficult. The input voltage-controlled technique is favorable with less computational intricacy, easy to implement, and provides good behavior for dynamic applications such as electric vehicles, pumping applications, etc., Compared to the above-mentioned techniques, vector control techniques such as intelligent control, current shaping technique, DTC and FOC provides good dynamic behavior on contrary to computational intricacy. Multi-level inverter topologies are also

recommended for both scalar and vector control schemes. The simulation results proving the most efficient control techniques and motor results are discussed in the upcoming sections.

VII. DESIGN PLATFORM FOR BLDC MOTOR

The design and development of high-performance BLDC motors for various applications are given in [136]. The technology used to develop the design optimum balanced solution of various factors like cost, power density, torque density, max speed, efficiency, simplicity for ease in manufacturing, etc., are discussed.

Designing of BLDC motor for light electric vehicle applications is carried out in this section. The 2 kW BLDC motor

design, analysis, and optimization techniques are using the following steps in Ansys software.

1. BLDC motor sizing
2. Motor architecture
3. Electromagnetics
   - 2D simulation
   - 3D simulation
4. Multiphysics simulations
   - Thermal
   - Structural
   - Modal
   - Computational fluid mechanics
5. Dyno testing

A. ELECTRO-MAGNETIC DESIGN
Selection of motor topology, slot-pole ratio, winding layout, Stator, and rotor geometry [137].

B. THERMAL DESIGN
Selection winding class, Varnish type, potting material selection. Design of cooling jacket based on accurate boundary conditions [138].

C. STRUCTURAL DESIGN
Analysing and optimizing stress concentration areas in various motor components. Calculation of various safety factors for structural components and improvising using geometry optimization [140].

D. NVH DESIGN
Model results simulation & Mode shapes validation at both component and assembly levels. Iterating various Slot-pole configurations to achieve an optimum natural frequency and sound pressure levels [139].

The motor sizing procedure starts from the drive duty cycle calculation based on vehicle speed rpm or motor speed. The diameter of the wheel and the height of the tire calculate the motor speed. Here, the motor can be designed concerning both the outer rotor and inner rotor for optimized geometry dimensions. The electromagnetic design was carried out 2D and 3D for analyzing all Multiphysics simulation parameters for both inner and outer rotors. The material Neodymium ferrite boron selected for rotor high-cost rare earth magnet has high coercivity, high energy density, and high remanence [141].

The M19-29grade non-oriented silicon steel material laminated in the stator side has a high energy density. The winding connected is whole coiled using Copper with minimum loss properties.

Motor width bottom, tooth width, back iron length, and slot depth the optimized geometry parameters are selected using several iterations that include different dimensions to get high performance, Multiphysics parameter simulation output for highly efficient and cost-effective prototype motor. Fig. 31 represents the various steps involved in designing
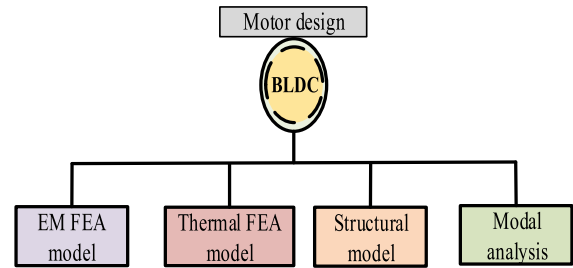
FIGURE 31. Motor design models.

TABLE 11. BLDC motor geometry dimension.

Motor geometry	Specifications
Speed	1000rpm
Rated Torque	16Nm
Outer Stator /inner rotor diameter	120/74mm
Outer Rotor /Inner stator diameter	140/120mm
Stack length	65mm
Number of slots	24
Stacking factor	0.95
Power rating	2kW
Voltage	60v
Current	37A
Rotor Magnet	NdFeB
Stator steel	M19-29G
Slot dimension	Optimized

and Fig. 32 represents the procedures involved in designing BLDC motor.

E. INNER ROTOR
The inner rotor BLDC motor inside is acting as rotor magnet mounted and stator winding is connected outside. The advantage of the inner rotor magnet is its ability to dissipate heat, lower inertia ratio, and ability to produce force impacts on heat [142]. The number of measurements was carried out both electrical and mechanical dimensions to fine-tune the data as shown in Table 11. The key dimensions to design both inner and outer BLDC are stator outer diameter, stator inner diameter, rotor outer diameter, rotor inner diameter, magnet thickness, airgap, and slot. The magnetic flux distribution and flux line pattern are shown in Fig. 33. The static and dynamic characteristics of the inner rotor are designed using Ansys FEA simulation for Multiphysics parameters. Maximum flux distribution is 1.66T when the rotor rotates 0 to 360 degrees measured in each position. The interaction between inner rotor rotation permanent magnet and stator slot coils results in maximum torque, rated torque, efficiency, core loss, power, flux pattern with speed characteristics transient condition.

The rotor position changes from the initial condition to attain the peak torque is 39 Nm. When the rotor position changes torque starts decreasing and at the rated speed it attains 16Nm.

From speed vs power characteristics, speed is increasing linearly, and when it reaches rated speed 1000rpm it reaches the maximum power of 2 kW. At very low speed the
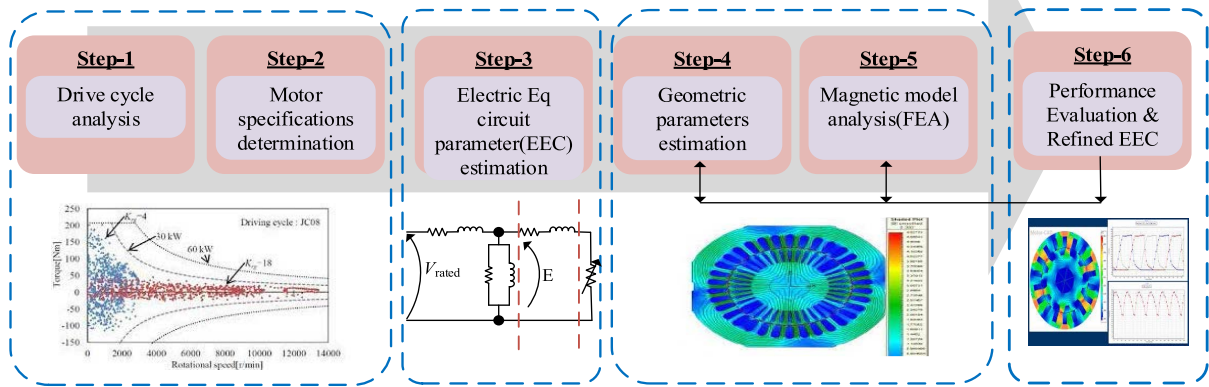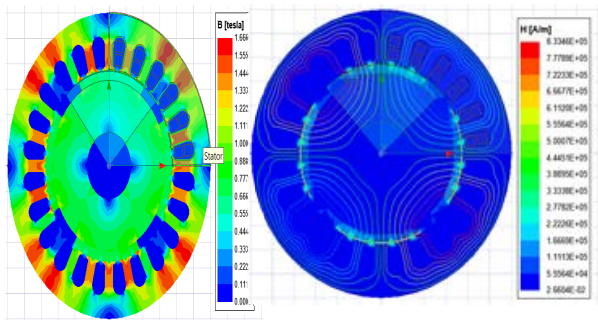
FIGURE 32. Motor design step by step procedure.

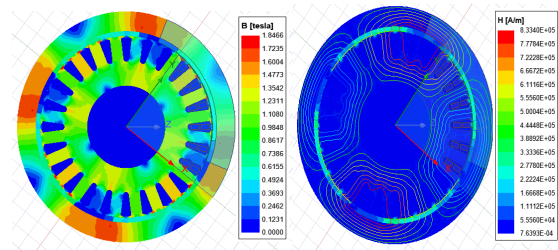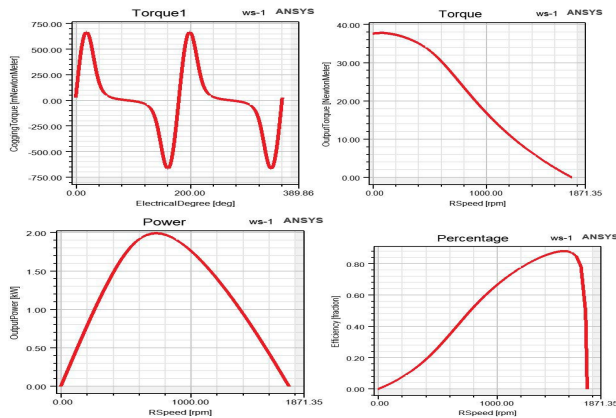**FIGURE 33.** Inner rotor flux distribution and magnetic flux lines.

FIGURE 34. Inner rotor cogging torque, torque, power, and efficiency.

efficiency starts to increase and it reaches a maximum of 88% at 1800rpm. For rated speed 1500 rpm, efficiency is 82% and core loss reduced maximum all are depicted in Fig. 34.

F. OUTER ROTOR (HUB MOTOR)
The outer rotor or in wheel motor stator slot winding is connected inside and the rotor magnet is mounted outside. The primary advantage of the hub motor is low cogging
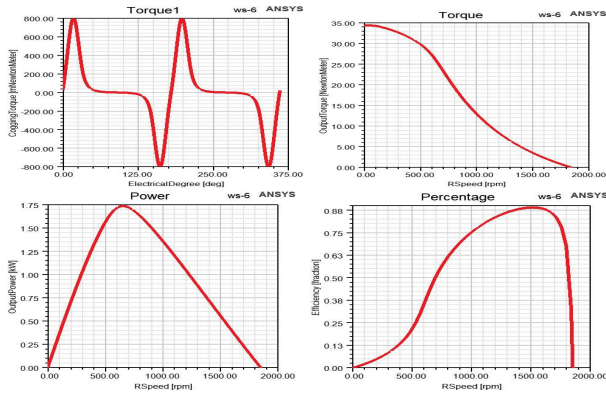

FIGURE 35. Outer rotor flux distribution and magnetic flux lines.

torque compared to the inner rotor. In the design aspect, the outer rotor when compared to the inner rotor, the minimum rated current or lower duty cycle occurs at rated speed. Maximum flux distribution is 1.86 Tesla when the rotor rotates from 0 to 360 degrees measured in each position as shown in Fig. 35 [143].

The optimized geometry simulation output waveform for the outer rotor is shown in Fig. 39. The rotation of motor rotor position is plotted between cogging torque and speed characteristics.

The geometry parameters are optimized for the same dimensions mentioned in Table 11. The interaction between outer rotor rotation permanent magnet and stator slots coils maximum torque, rated torque, efficiency, core loss, power, flux pattern with speed characteristics transient conditions is discussed in [144]. The outer rotor cogging torque vs rotor rotation speed, and the outer rotor magnet cogging torque is very low compared to inner rotor torque as shown in Fig. 36.

In output torque vs rotor position graph, at the initial rotor start position, the torque reaches a maximum is 35 Nm. When the rotor changes the initial position, speed starts to increase as rated torque decreases, it reaches 14 Nm at a rated speed of 1000 rpm. In the output power vs rotor speed characteristics at a rated speed of 1000 rpm, the power reaches 1.75 kW. In the efficiency vs rotor position speed, at rated 1000 rpm the efficiency reaches 88% and comparison results of main parameters are listed in Table 12.

FIGURE 36. Outer rotor cogging torque, torque, power, and efficiency.

TABLE 12. FEA simulation results BLDC 2 kW, 1000 rpm.

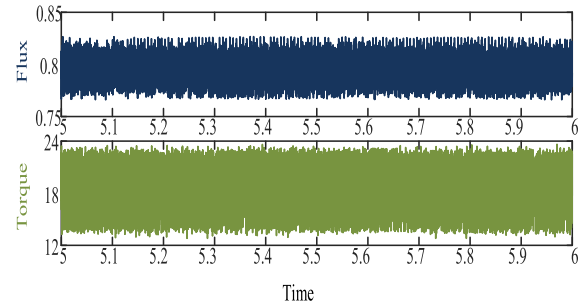| Rotor structure	Cogging torque	Efficiency%
Inner rotor	High	83
Outer rotor	Low	88
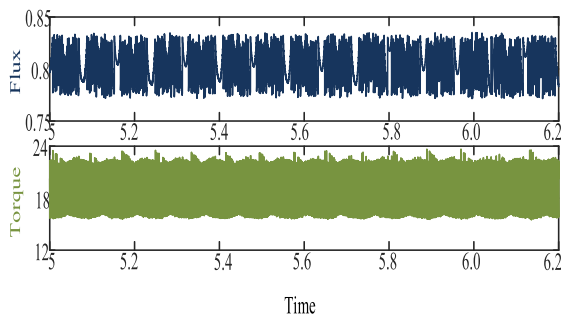
FIGURE 37. FOC fed Torque and flux response at 500 rpm.

FIGURE 38. FOC fed torque and flux response at 1000 rpm.
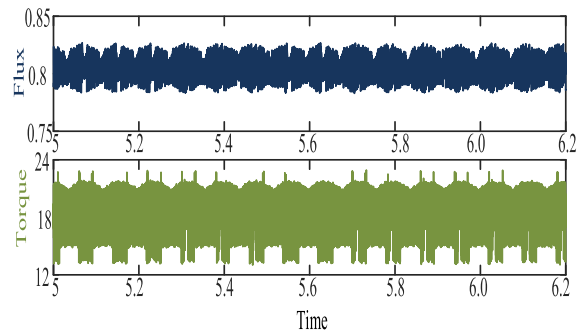
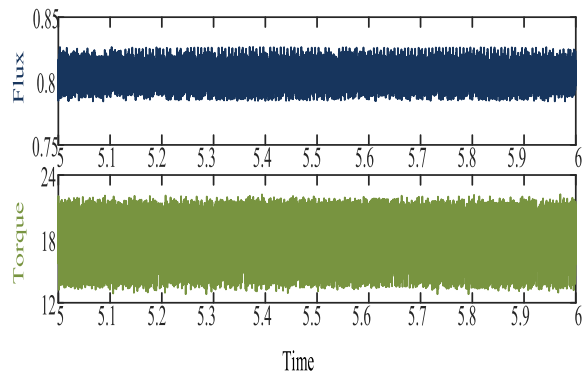**FIGURE 39.** DTC fed torque and flux response at 500 rpm.

FIGURE 40. DTC fed torque and flux response at 1000 rpm.

VIII. CONTROL TECHNIQUES SIMULATION RESULTS

The simulation results of various control algorithms such as FOC, DTC, and intelligent control are verified using MATLAB software and results are discussed as follows. The speed parameters are varied to show the difference in results obtained.

The features of FOC, DTC, and Intelligent control techniques are compared. And found that intelligent control schemes are more efficient compared to other techniques. In intelligent control schemes: (i) *dq* vector transformation is obviated, (ii) No traditional PWM algorithms are applied, (iii) hysteresis controllers aren't used as indirect torque control, and (iv) switching frequency is reduced compared to other control schemes. The FOC control strategy results are shown in Fig. 37 and Fig. 38. BLDC flux and torque are obtained at 500 rpm, and 1000 rpm respectively. The torque reference is maintained as 15 Nm during the whole simulation.

The DTC control strategy results are shown in Fig. 39 and Fig. 40. BLDC flux and torque are obtained at 500 rpm, and

1000 rpm respectively. The torque reference is maintained as 15 Nm during the whole simulation.

The Intelligent control strategy results are shown in Fig. 41 and Fig. 42. BLDC flux, speed, and torque are obtained at 500 rpm, and 1000 rpm respectively. The torque reference is maintained as 15 Nm during the whole simulation.

Table 13, 14, 15 represent the results and discussion of torque ripples, flux ripples, and current THD of FOC, DTC, and Intelligent control. The results are obtained as standard deviation values. Thus, proving that the intelligent control technique is more efficient compared to other techniques.

IX. BLDC MOTOR HARDWARE RESULTS

The hardware analysis, performance, and designing of the BLDC motor controller using vector control is done and
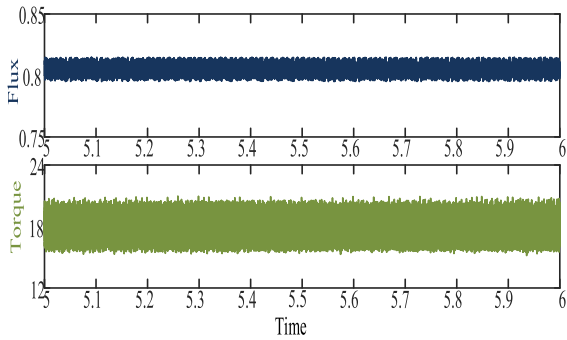
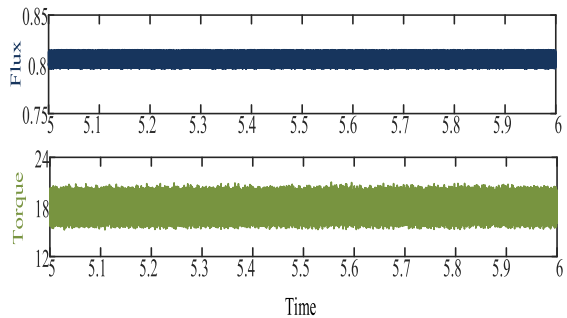**FIGURE 41. Intelligent control fed torque and flux response at 500 rpm.**

FIGURE 42. Intelligent control fed Torque and flux response at 1000 rpm.

TABLE 13. Results of FOC.

Speed	FOC		
	Torque ripples	Flux ripples	Current THD
500	1.885	1.0005	16.35
1000	2.005	0.0093	16.61

TABLE 14. Results of DTC.

Speed	DTC		
	Torque ripples	Flux ripples	Current THD
500	1.561	0.0089	15.05
1000	1.774	0.0082	15.93

TABLE 15. Results of intelligent control.

Speed	Intelligent Control		
	Torque ripples	Flux ripples	Current THD
500	1.091	0.0065	11.67
1000	1.074	0.0066	12.01

the results are verified with help of Altair embed software. The parameters used for the field orientation control simulation are shown in Table 16. To optimize the output, the proportional-integral controller parameters K_p are changed from 0.04474 s to 0.015 ms and K_i to 0.04474 ms. These Altair embed results are obtained during 500 and 1000 rpm of the motor.

The proposed experiment hardware platform is shown in Fig. 43 which includes a BLDC motor, regulated power supply, Altair embed software, mixed scale oscilloscope, and DRV C2-H2 motor controller which uses TMS320F280 DSP as a microcontroller. This Altair embed software is an emulator which can be used for coding various microcontrollers using visual simulation.

TABLE 16. Motor controller parameters.

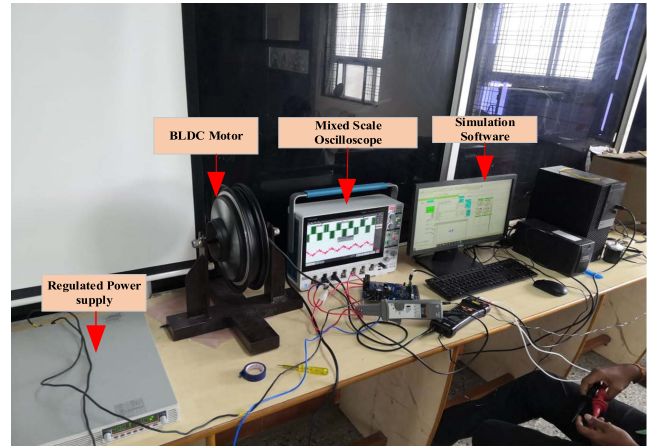| Parameters	Values
Supply voltage (V_{dc})	48 V
Motor voltage	48 V
poles	4
Stator inductance	10.5e-3 H
Mutual inductance	1H
Stator Resistance	1.12 Ω
Power ratings	250 W
Current reference	0.7

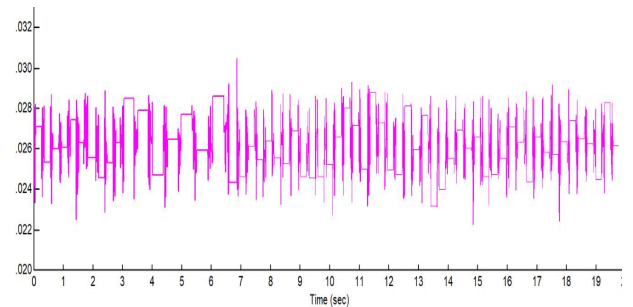**FIGURE 43. Hardware BLDC hub type motor setup.**

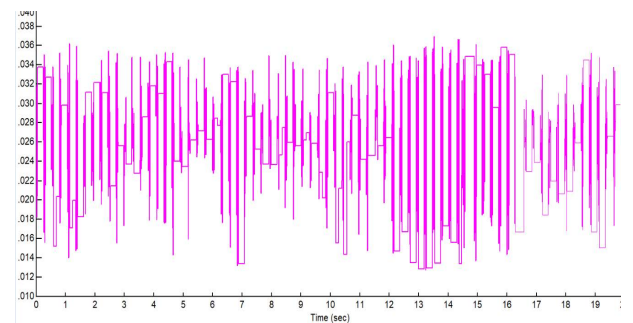**FIGURE 44. Vector switching states at low speed.**

FIGURE 45. Vector switching states at high speed.

The vector switching states at various speed conditions are shown in Fig. 44 and Fig. 45. From the above results, it is inferred that the analyzed vector control technique produces minimum vector switching state transition. And hence the operation happens with less switching frequency.
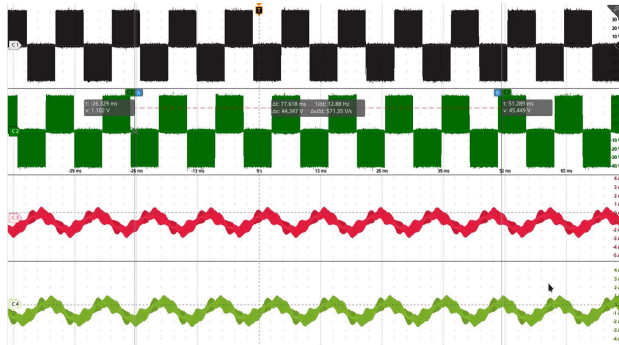
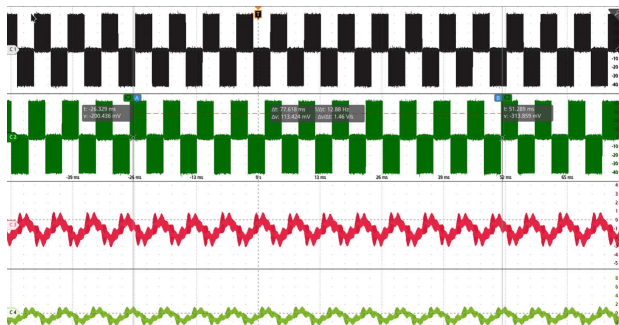**FIGURE 46.** Phase current and line-line voltage waveform at medium speed

FIGURE 47. Phase current and line-line voltage waveform at High speed.
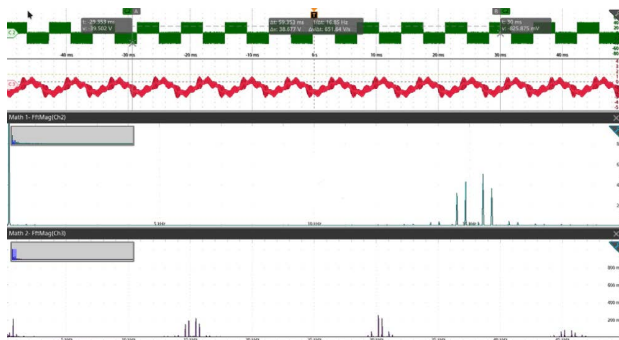

FIGURE 48. Current THD and Voltage THD generation.

The motor back EMF and phase current results are obtained from the analyzed vector control topology by changing the speed of the BLDC motor from 500 rpm and 1000 rpm and shown in Fig. 47 and Fig. 48. From the obtained results, we can observe that the vector control technique provides a good response. From the hardware results, we can infer that during the change in speed the frequency of the switching operation is also varied. The current THD and voltage THD results of the analyzed vector control scheme are shown in Fig. 52. Since the switching frequency of the proposed operation is 15 kHz, the current THD and voltage THD is observed at 15 kHz. The voltage THD value rises to 4 volts and the current THD value rises to 200 mA. Hence the obtained hardware results provide a good response over various conditions and the THD values are less for the smooth operation of the machine. Table 17 depicts the torque ripple, flux ripple, and THD generated by the proposed

TABLE 17. Hardware results of vector control.

Speed	Field oriented control			
	Torque ripples	Flux ripples	Current THD	Average switching frequency
500	2.965	2.051	23.35	1.712
1000	3.625	3.256	26.16	1.914

algorithm. The values are obtained as standard deviation values. In the upcoming sections, the future scopes of BLDC motor researches are discussed from the result findings.

X. FUTURE CHALLENGES AND OPPORTUNITIES
A. LITERATURE WORK
The BLDC motor designing, and the analysis of BLDC motor controllers are discussed in this paper. During the initial stages, BLDC motors were controlled using scalar control techniques. Nowadays researchers prefer vector control techniques such as FOC, DTC, and intelligent control techniques such as PSO optimization, MPC, etc., These techniques provide good response over various static and dynamic conditions and produce less torque and flux ripples. These vector control techniques increase the structural and computational complexity which is realized that these vector control techniques are practically difficult [145].

Thus, nowadays researchers are trying to reduce these complexities. Researchers are trying to reduce the generated torque and flux ripple generated in each vector control technique such as controlling input voltage, current shaping techniques, and drive inverter topology [146]. In controlling the input voltage technique, researchers are trying to reduce the torque ripples by reducing the spikes in DC-DC converter output, and in the PWM-based technique, as well as to use the space vector PWM technique with more vectors. In the current shaping technique researchers are trying to improve the response of the drive-by excluding the hysteresis controller. In the conventional drive inverter topology-based research papers, 3L-neutral point clamped inverters are controlled using the scalar control technique, and Z-source inverters are used to reduce the torque ripples [147]. Nowadays, researchers are trying to reduce the torque ripples of 3L-NPC MLI by using MCPWM and SVPWM techniques for BLDC motors.

B. FUTURE TRENDS
- The motor vibrations and torque ripple of the BLDC motor should be reduced significantly without obvious torque decline and reduction inefficiency.
- Reducing the cost of the BLDC motor using alternate ferrite magnet material to improve efficiency.
- Analysis of control schemes should be improved for a wide speed range.
- Hybrid control topologies such as Predictive torque control and DTC clubbed or predictive current control and FOC should be developed and analysed.

TABLE 18. Review of various torque ripple mitigation techniques.

Ref	Advanced control technique	Inference
[148]	Field orientation control	An indirect FOC control scheme is designed which uses a back EMF structure for controlling the flux parameters. This developed control algorithm is used for UAVs.
[149]	Direct torque control	The DTC developed the maximum torque per ampere concept for controlling the control variables. The iron loss concepts in BLDC motors are excluded while controlling the variables.
[150]	Current shaping technique	A predictive current control technique is discussed where current control is achieved by injecting square phase current through the control algorithm ensuring maximum torque per ampere.
[151]	Controlling input voltage	Quadral-duty digital PWM-based pulses are generated to control the inverter part of the motor controller which efficiently controls the torque and flux parameters of the BLDC motor.
[152]	Intelligent control	A BLDC motor controller is designed in which the outer torque controller is developed with the help of a model predictive algorithm. The designed control algorithm works in offline mode.
[153]	Drive inverter topology	A torque ripple reduction concept is discussed with help of NPCMLI and SEPIC converter. T-shaped NPC MLI are discussed and the effects are analyzed.
[154]	Fault tolerance control	A model-based FTC topology is discussed for the BLDC motor drive system. Open switch fault control is concentrated and the control algorithm is discussed for online mode.
[155]	Electromagnetic interference.	The effect of load parasitic on common-mode conducted elements is analyzed. While analyzing bipolar PWM operated BLDC motors are taken into account

- Direct torque control topology can be developed with help of reference voltage vectors for BLDC motor and its complexity can be reduced.
- Multi-level inverter topologies can be developed using vector control technique for BLDC motor.
- BLDC motor drives can be developed with SVPWM and MLI concepts. SVPWM concepts can be initiated with fewer vectors.
- Intelligent control concepts can be developed with less complexity by reducing the torque and flux control vectors in control schemes.
- BLDC motor controllers should be developed in such a manner that it produces less torque ripple during faulty conditions with extra power switches.
- Bearing current reduction can be given more importance while discussing EMI reduction for BLDC motor drive system
- FTC algorithm for inverter multiple switch tube problems should be approached.
- FTC based Artificial neural network algorithm must be discussed for various faults such as stator intern fault and demagnetization fault.

XI. CONCLUSION

The automobile industry is migrating towards eco-friendly transportation with less pollution, hence attention towards electric vehicles and hybrid electric vehicles is increasing. BLDC motors are gaining more interest in EV applications due to their simple, robust, and high-efficiency ability. This paper reviews various types of BLDC motors, their standards, applications, torque ripple mitigation techniques, and BLDC motor control techniques, in addition to a discussion on the development of a design platform for BLDC motors. A current study reveals that,

- Currently, outer surface rotor-type BLDC motors such as Hub motors are used widely for commercial applications.
- The BLDC motor control drive is used to overcome fault-tolerant control, electromagnetic interference control, and acoustic noise control techniques are discussed.
- Outer surface rotor-type motors are more popular due to the minimum cogging torque leading to high loading effect, high power, and increased efficiency. These motors have a lower requirement of cooling for the rotor as they are exposed to the outer atmosphere receiving ambient air cooling.
- Torque ripples in BLDC motors are more at low speeds and less at high speeds. However, Axial-type BLDC motors have higher efficiency and higher torque than the other types of EV motors. Hub motor is used in EV due to its advantage of compact size and retrofitting type model.
- Intelligent controller stands superior amongst the various control techniques used for BLDC motors as it reduces torque ripples better than the other types of controllers.
- Design and FEA analysis of an inner rotor type BLDC motor and an outer rotor type BLDC motor have been presented in this paper. The simulation results substantiate the effectiveness of the outer surface rotor-type BLDC motor. Hardware results also confirm the simulation results.
- Finally, the challenges in BLDC motor current control techniques and future opportunities are discussed for future researchers.

APPENDIX

A_c = cross-sectional area of a conductor in mm
A_{cu} = area of a copper conductor in a slot in m^2
B_g = Air gap flux density in the middle 120^0 of a poles Wb/m^2
B_{max} = Maximum flux density in Wb/m^2
D_c = Diameter of the conductor in mm
d_s = slot depth in mm
D_{steel} = Density of steel in kg/m^3
E_b = Back EMF of the motor in volts
E_c = EMF induced per conductor in volts
E_t = EMF induced in a turn in volts
g = air gap in mm
I_c = current through a conductor in amps
I_{phase} = phase current in amps.

I_s = current in a DC source in amps
J = maximum current density in Amps/m^2
K_{fill} = slot fill factor
L = active length of the motor in mm
l_t = length of turn in m
N_{ph} = several phases.
n_s = total number of turns in a slot
N_s = number of slots
P = number of poles
$P_{loss\ cu}$ = copper loss in watts
$P_{loss\ core}$ = core loss in watts
$\phi_{\tau s}$ = flux in slot pitch in Wb.
ϕ_t = flux in the tooth in Wb
ρ_{cu} = resistivity of copper in ohm-cm
R_{ph} = Resistance of phase in ohms.
R_{ro} = Rotor outer radius in mm.
R_{si} = stator inner radius in mm.
R_{so} = stator outer radius in mm.
R_t = Resistance of a turn in ohms
SPP = slot pole phase.
τ_c = coil pitch.
τ_s = slot pitch.
V = linear velocity of a rotor in m/sec.
V_{cu} = volume of copper in m^3.
V_{rotor} = volume of the rotor in m^3.
V_{stator} = volume of stator in m^3.
w_{bi} = back iron length in mm
w_{cu} = weight of copper in Kg
ω_m = Angular velocity of the rotor in m/sec
W_{motor} = weight of motor in Kg
$W_{stator/rotor}$ = Weight of stator/ rotor in Kg
W_t = tooth width in mm

A. DESIGN BLDC MOTOR TORQUE EQUATION

Force on a current-carrying conductor in a magnetic field

$$F = IL * B$$
$$F = BIL \sin \theta$$

Force on one conductor

$$F_c = B_g I_c L$$

Torque on one turn

$$T_c = B_g I_c L R_{si}$$

Torque on one coil

$$T_t = 2B_g I_c L R_{si}$$
$$T_{coil} = 2B_g I_c n_s L R_{si}$$

Torque on one phase

$$T_{phase} = 2\rho B_g I_c n_s L R_{si}$$

Torque developed in Motor

$$T = 2 * 2p B_g I_c n_s L R_{si}$$
$$I_c = I_{phase} = I_s$$

$$T = 2P B_g I_c n_s L R_{si}$$

Therefore P = 2p

L -Length of the conductor
B- Magnetic flux density
I-Current through conductor
θ- Angle between L and B

B. BLDC BACK EMF EXPRESSION

EMF in one conductor

$$E_c = B_g L v$$
$$E_c = B_g L w_m R_{si}$$

EMF in one turn

$$E_t = 2B_g L w_m R_{si}$$

EMF in one Coil

$$E_{coil} = 2B_g L n_s W_m R_{si}$$

EMF in one phase

$$E_{phase} = P B_g L n_s W_m R_{si}$$

Back EMF in BLDC motor

$$E_b = 2P B_g L n_s W_m R_{si}$$

C. STATOR WINDING DESIGN

Maximum current density in a conductor

$$A_c = \frac{I_c}{j}; \quad D_c = 2\sqrt{\frac{A_c}{\pi}}$$

Coil pitch

$$\tau_c = \frac{2\pi \left(R_{si} + \frac{1}{2}d_s\right) l}{P}$$
$$l_t = 2L + 2\tau_c$$

D. STATOR SLOT DESIGN

Slot area

$$A_s = \frac{A_{cu}}{K_{fill}}$$

Slot fill factor

$$R_{ro} = R_{si} - g; \quad N_s = P * N_{ph}$$
$$\tau_s = \frac{2\pi R_{si}}{N_s}$$

Slot pitch

$$\phi_{\tau s} = \phi_t$$
$$\tau_s L B_g = w_t L B_{max}$$

Trapezoidal slot area

$$W_t = \frac{B_g}{B_{max}}\tau_s; \quad w_{sb} = \tau_s - w_t$$

$$A_s = \frac{1}{2}(w_{st} + w_{sb}) * d_s$$

$$w_{st} = \frac{2\pi(R_{si} + d_s)}{N} - w_t$$

Stator back iron

$$\frac{2\pi R_{si}}{2p} LB_g = w_{bi}LB_{\max}; \quad w_{bi} = \frac{B_g \pi R_{si}}{B_{\max}P}$$

$$R_{so} = R_{si} + d_s + w_{bi}$$

Weight of the BLDC motor

Rotor

$$V_{rotor} = \pi R_{ro}^2 L$$

$$W_{rotor} = D_{steel} * V_{rotor}$$

Stator

$$V_{stator} = \pi\left(R_{so}^2 - R_{si}^2\right)L - N_s A_s L$$

$$W_{stator} = D_{steel} * V_{stator}$$

Windings

$$V_{cu} = N_{ph}pn_s l_t A_c$$

$$W_{cu} = D_{cu} * V_{rotor}$$

Overall weight

$$W_{motor} = W_{rotor} + W_{stator} + W_{cu}$$

$$R_t = \frac{\rho_{cu} l_t}{A_c}; \quad R_{ph} = \rho n_s R_t$$

E. BLDC LOSSES

Copper losses

$$P_{loss\ cu} = 2 I_s^2 R_{ph}$$

Core losses

$$P_{loss\ core} = (coreloss/Kg) * W_{stator}$$

REFERENCES

[1] H.-W. Kim, K.-T. Kim, Y.-S. Jo, and J. Hur, "Optimization methods of torque density for developing the neodymium free SPOKE-type BLDC motor," *IEEE Trans. Magn.*, vol. 49, no. 5, pp. 2173–2176, May 2013, doi: 10.1109/TMAG.2013.2237890.

[2] J. Shao, "An improved microcontroller-based sensor less brushless DC (BLDC) motor drive for automotive applications," *IEEE Trans. Ind. Appl.*, vol. 42, no. 5, pp. 1216–1221, Sep. 2006.

[3] J. Shao, "An improved microcontroller-based sensorless brushless DC (BLDC) motor drive for automotive applications," in *Proc. 40th IAS Annu. Meeting. Conf. Rec. Ind. Appl. Conf.*, Oct. 2005, pp. 2512–2517.

[4] C. L. Xia, *Permanent Magnet Brushless DC Motor Drives and Controls*. Singapore: Wiley, 2012.

[5] K. P. Kumar, "Modeling of a commercial BLDC motor and control using GA- controller for a BLDC propulsion application for hybrid electric vehicle," *Int. J. Psychosocial Rehabil.*, vol. 23, no. 4, pp. 1604–1613, Dec. 2019.

[6] A. Senthilnathan and P. Palanivel, "Fuzzy logic controller based zeta converter for BLDC motor," *J. Adv. Res. Dyn. Control Syst.*, vol. 12, no. 7, pp. 125–133, Jul. 2020.

[7] H.-J. Kim, "BLDC motors for robot vacuum cleaners," *Trans. Korean Inst. Electr. Eng.*, vol. 60, no. 4, pp. 172–174, Dec. 2011.

[8] J. W. K. K. Jayasundara and R. Munasinghe, "Software design tool for optimum axial flux BLDC motors," in *Proc. Int. Conf. Ind. Inf. Syst. (ICIIS)*, Dec. 2009, pp. 526–531.

[9] G. Sotyaramadhani, A. Wikarta, and M. N. Yuniarto, "Different approach of fuzzy logic algorithm implementation for increasing performance of axial BLDC motor," in *Proc. AIP Conf.*, 2018, Art. no. 060010.

[10] S. De, M. Rajne, S. Poosapati, C. Patel, and K. Gopakumar, "Low inductance axial flux BLDC motor drive for more electric aircraft," in *Proc. Aerosp. Conf.*, Mar. 2011, pp. 1–11, doi: 10.1109/AERO.2011.5747464.

[11] E. Yeşilbağ, Y. Ertuğrul, and L. Ergene, "Axial flux PM BLDC motor design methodology and comparison with a radial flux PM BLDC motor," *TURKISH J. Electr. Eng. Comput. Sci.*, vol. 25, pp. 3455–3467, 2017.

[12] S. Sakunthala, R. Kiranmayi, and P. N. Mandadi, "A study on industrial motor drives: Comparison and applications of PMSM and BLDC motor drives," in *Proc. Int. Conf. Energy, Commun., Data Anal. Soft Comput. (ICECDS)*, Aug. 2017, pp. 537–540, doi: 10.1109/ICECDS.2017.8390224.

[13] G. D. Donato, G. Scelba, M. Pulvirenti, G. Scarcella, and F. G. Capponi, "Low-cost, high-resolution, fault-robust position and speed estimation for PMSM drives operating in safety-critical systems," *IEEE Trans. Power Electron.*, vol. 34, no. 1, pp. 550–564, Jan. 2019.

[14] Y. Ming and J.-X. Shen, "Research on conducted EMI and vibration characteristics of PM BLDC motors with different stator structures," in *Proc. Int. Conf. Electr. Mach. Syst.*, Aug. 2011, pp. 1–6, doi: 10.1109/ICEMS.2011.6073454.

[15] A. Tashakori and M. Ektesabi, "A simple fault tolerant control system for Hall effect sensors failure of BLDC motor," in *Proc. IEEE 8th Conf. Ind. Electron. Appl. (ICIEA)*, Jun. 2013, pp. 1011–1016.

[16] M. Perotti, "On the influence of the load parasitics on the CM conducted EMI of BLDC motor drives," in *Proc. IEEE Int. Conf. Environ. Electr. Eng. Ind. Commercial Power Syst. Eur. (EEEIC/I&CPS Eur.)*, Jun. 2020, pp. 1–6, doi: 10.1109/EEEIC/ICPSEurope49358.2020.9160663.

[17] G. Buja, M. Bertoluzzo, and R. K. Keshri, "Torque ripple-free operation of PM BLDC drives with petal-wave current supply," *IEEE Trans. Ind. Electron.*, vol. 62, no. 7, pp. 4034–4043, Jul. 2015, doi: 10.1109/TIE.2014.2385034.

[18] A. Darba, F. D. Belie, P. D'haese, and J. A. Melkebeek, "Improved dynamic behavior in BLDC drives using model predictive speed and current control," *IEEE Trans. Ind. Electron.*, vol. 63, no. 2, pp. 728–740, Feb. 2016, doi: 10.1109/TIE.2015.2477262.

[19] S.-K. Lee, G.-H. Kang, J. Hur, and B.-W. Kim, "Stator and rotor shape designs of interior permanent magnet type brushless DC motor for reducing torque fluctuation," *IEEE Trans. Magn.*, vol. 48, no. 11, pp. 4662–4665, Nov. 2012.

[20] M. A. N. Doss, S. Jeevananthan, S. S. Dash, and M. J. Hussain, "Critical evaluation of cogging torque in BLDC motor with various techniques," *Int. J. Autom. Control*, vol. 7, pp. 135–146, Jan. 2013.

[21] A. M. Doss, M. Ramasamy, and M. S. Karthikeyan, "Cogging torque reduction in brushless dc motor by reshaping of rotor magnetic poles with grooving techniques," *Int. J. Appl. Eng. Res.*, vol. 10, no. 36, pp. 27781–27785, 2015.

[22] Z. Guo, L. Chang, and Y. Xue, "Cogging torque of permanent magnet electric machiens: An overview," in *Proc. Can. Conf. Electr. Comput. Eng.*, May 2009, pp. 1172–1177, doi: 10.1109/CCECE.2009.5090310.

[23] G. Liu, C. Cui, K. Wang, B. Han, and S. Zheng, "Sensorless control for high-speed brushless DC motor based on the Line-to-Line back EMF," *IEEE Trans. Power Electron.*, vol. 31, no. 7, pp. 4669–4683, Jul. 2016.

[24] A. Ahfock and D. Gambetta, "Sensorless commutation of printed circuit brushless direct current motors," *IET Electr. Power Appl.*, vol. 4, no. 6, pp. 397–406, Jul. 2010.

[25] T. Yazdan, W. Zhao, T. A. Lipo, and B.-I. Kwon, "A novel technique for two-phase BLDC motor to avoid demagnetization," *IEEE Trans. Magn.*, vol. 52, no. 7, pp. 1–4, Jul. 2016, doi: 10.1109/TMAG.2016.2521874.

[26] G. Haines and N. Ertugrul, "Wide speed range sensorless operation of brushless permanent-magnet motor using flux linkage increment," *IEEE Trans. Ind. Electron.*, vol. 63, no. 7, pp. 4052–4060, Jul. 2016.

[27] J. Shao, "An improved microcontroller-based sensor less brushless DC (BLDC) motor drive for automotive applications," *IEEE Trans. Ind. Appl.*, vol. 42, no. 5, pp. 1216–1221, Sep./Oct. 2006.

[28] S.-T. Jo, H.-S. Shin, Y.-G. Lee, J.-H. Lee, and J.-Y. Choi, "Optimal design of a BLDC motor considering three-dimensional structures using the response surface methodology," *Energies*, vol. 15, no. 2, p. 461, Jan. 2022.

[29] T.-Y. Lee, M.-K. Seo, Y.-J. Kim, and S.-Y. Jung, "Motor design and characteristics comparison of outer-rotor-type BLDC motor and BLAC motor based on numerical analysis," *IEEE Trans. Appl. Supercond.*, vol. 26, no. 4, pp. 1–6, Jun. 2016, doi: 10.1109/TASC.2016.2548079.

[30] R. K. Behera, R. Kumar, S. M. Bellala, and P. Raviteja, "Analysis of electric vehicle stability effectiveness on wheel force with BLDC motor drive," in *Proc. IEEE Int. Conf. Ind. Electron. Sustain. Energy Syst. (IESES)*, Jan. 2018, pp. 195–200, doi: 10.1109/IESES.2018.8349873.

[31] I.-S. Jung, H.-G. Sung, Y.-D. Chun, and J.-H. Borm, "Magnetization modeling of a bonded magnet for performance calculation of inner-rotor type BLDC motor," *IEEE Trans. Magn.*, vol. 37, no. 4, pp. 2810–2813, Jul. 2001, doi: 10.1109/20.951314.

[32] A. Damiano, A. Floris, G. Fois, I. Marongiu, M. Porru, and A. Serpi, "Design of a high-speed ferrite-based brushless DC machine for electric vehicles," *IEEE Trans. Ind. Appl.*, vol. 53, no. 3, pp. 4279–4287, Sep./Oct. 2017, doi: 10.1109/TIA.2017.2699164.

[33] R. Qu and T. A. Lipo, "Dual-rotor, radial-flux, torodially wound, permanent-magnet machines," *IEEE Trans. Ind. Appl.*, vol. 39, no. 6, pp. 1665–1673, Nov. 2003.

[34] R. Qu and T. A. Lipo, "Design and parameter effect analysis of dual-rotor, radial-flux, toroidally wound, permanent-magnet machines," *IEEE Trans. Ind. Appl.*, vol. 40, no. 3, pp. 771–779, May 2004.

[35] R. Qu and T. A. Lipo, "Design and optimization of dual-rotor, radial-flux, toroidally-wound, permanent-magnet machines," in *Proc. 38th IAS Annu. Meeting Conf. Rec. Ind. Appl. Conf.*, Nov. 2003, pp. 1397–1404.

[36] R. Qu and T. A. Lipo, "Analysis and modeling of air gap and zigzag leakage fluxes in a surface-mounted-PM machine," in *Proc. 37th IAS Annu. Meeting*, Feb. 2002, pp. 2507–2513.

[37] S. H. Lee, S. B. Park, S. O. Kwon, J. Y. Lee, J. J. Lee, J. P. Hong, and J. Hur, "Characteristic analysis of the slotless axial-flux type brushless DC motors using image method," *IEEE Trans. Magn.*, vol. 42, no. 4, pp. 1327–1330, Apr. 2006, doi: 10.1109/TMAG.2006.871922.

[38] L. Yang, J. Zhao, X. Liu, A. Haddad, J. Liang, and H. Hu, "Comparative study of three different radial flux ironless BLDC motors," *IEEE Access*, vol. 6, pp. 64970–64980, 2018, doi: 10.1109/ACCESS.2018.2878267.

[39] E. Bostanci, Z. Neuschl, and R. Plikat, "Influence of phase magnetic couplings on phase current characteristics of multiphase BLDC machines with overlapping phase windings," *IEEE Trans. Magn.*, vol. 51, no. 9, pp. 1–13, Sep. 2015, doi: 10.1109/TMAG.2015.2430833.

[40] S. H. Lee, S. B. Park, S. O. Kwon, J. Y. Lee, J. J. Lee, J. P. Hong, and J. Hur, "Characteristic analysis of the slotless axial-flux type brushless DC motors using image method," *IEEE Trans. Magn.*, vol. 42, no. 4, pp. 1327–1330, Apr. 2006, doi: 10.1109/TMAG.2006.871922.

[41] H. Jin, G. Liu, and S. Zheng, "Commutation error closed-loop correction method for sensorless BLDC motor using hardware-based floating phase back-EMF integration," *IEEE Trans. Ind. Informat.*, vol. 18, no. 6, pp. 3978–3986, Jun. 2022, doi: 10.1109/TII.2021.3113368.

[42] S. Tsotoulidis and A. N. Safacas, "Deployment of an adaptable sensorless commutation technique on BLDC motor drives exploiting zero sequence voltage," *IEEE Trans. Ind. Electron.*, vol. 62, no. 2, pp. 877–886, Feb. 2015.

[43] W. Chen, H. Liu, X. Gu, X. Li, and T. Shi, "A position sensorless control strategy for brushless DC motor based on the back-electromotive force function," *IEEE Trans. Ind. Electron.*, vol. 34, no. 22, pp. 4661–4669, Jan. 2019.

[44] P. Damodharan and K. Vasudevan, "Sensorless brushless DC motor drive based on the zero-crossing detection of back electromotive force (EMF) from the line voltage difference," *IEEE Trans. Energy Convers.*, vol. 25, no. 3, pp. 661–668, Sep. 2010.

[45] X. Zhou, Y. Zhou, C. Peng, F. Zeng, and X. Song, "Sensorless BLDC motor commutation point detection and phase deviation correction method," *IEEE Trans. Power Electron.*, vol. 34, no. 6, pp. 5880–5892, Jun. 2019.

[46] T.-Y. Ho, "The design of motor drive for brushless DC motor," in *Electric Machines for Smart Grids Applications—Design, Simulation and Control*. London, U.K.: Intech Open, Dec. 2018, doi: 10.5772/intechopen.78815.

[47] W. Fan and T. Chen, "Design and implementation of fuzzy PID controller for brushless DC motor control system," *Appl. Mech. Mater.*, vol. 432, pp. 472–477, Sep. 2013.

[48] G. Guruvareddiyar and B. Subathra, "An open and short circuit switch fault of power converters in PM-BLDC motor in electric vehicle," in *Proc. IEEE Int. Conf. Clean Energy Energy Efficient Electron. Circuit Sustain. Develop. (INCCES)*, Dec. 2019, pp. 1–3.

[49] K. Karthik, R. K. Kumar, and P. Sreenivasulu, "Modeling and performance analysis of BLDC motor under different operating speed conditions," *Int. J. Eng. Comput. Sci.*, vol. 6, pp. 21468–21475, Jun. 2017.

[50] D. G. Dorrell, "A review of the methods for improving the efficiency of drive motors to meet IE4 efficiency standards," *J. Power Electron.*, vol. 14, no. 5, pp. 842–851, Sep. 2014.

[51] A. Nami, "Power electronics for future power grids: Drivers and challenges," in *Proc. 20th Eur. Conf. Power Electron. Appl. (EPE ECCE Eur.)*, Sep. 2018, p. 1.

[52] O. Tosun, N. F. O. Serteller, and G. Yalcin, "Comprehensive design and optimization of brushless direct current motor for the desired operating conditions," in *Proc. 25th Int. Conf. Electron.*, Jun. 2021, pp. 1–6, doi: 10.1109/IEEECONF52705.2021.9467459.

[53] B. V. R. Kumar and K. S. Kumar, "Design of a new dual rotor radial flux BLDC motor with Halbach array magnets for an electric vehicle," in *Proc. IEEE Int. Conf. Power Electron., Drives Energy Syst. (PEDES)*, Dec. 2016, pp. 1–5.

[54] V. Bogdan, M. Adrian, L. Leonard, B. Alexandra, S. Alecsandru, and N. Ionut, "Design and optimization of a BLDC motor for small power vehicles," in *Proc. Int. Conf. Electromech. Energy Syst. (SIELMEN)*, Oct. 2021, pp. 438–443, doi: 10.1109/SIELMEN53755.2021.9600327.

[55] T. A. Anuja and M. A. N. Doss, "Reduction of cogging torque in surface mounted permanent magnet brushless DC motor by adapting rotor magnetic displacement," *Energies*, vol. 14, no. 10, p. 2861, May 2021, doi: 10.3390/en14102861.

[56] L. Zhai, L. Lin, X. Zhang, and C. Song, "The effect of distributed parameters on conducted EMI from DC-fed motor drive systems in electric vehicles," *Energies*, vol. 10, no. 1, p. 1, Dec. 2016, doi: 10.3390/en10010001.

[57] A. Usman and B. S. Rajpurohit, "Time-efficient fault diagnosis of a BLDC motor drive deployed in electric vehicle applications," in *Proc. IEEE Global Humanitarian Technol. Conf. (GHTC)*, Oct. 2020, pp. 1–5, doi: 10.1109/GHTC46280.2020.9342941.

[58] A. Khazaee, H. A. Zarchi, G. A. Markadeh, and H. Mosaddegh Hesar, "MTPA strategy for direct torque control of brushless DC motor drive," *IEEE Trans. Ind. Electron.*, vol. 68, no. 8, pp. 6692–6700, Aug. 2021, doi: 10.1109/TIE.2020.3009576.

[59] D. Lu, J. Li, M. Ouyang, and J. Gu, "Research on hub motor control of four-wheel drive electric vehicle," in *Proc. IEEE Vehicle Power Propuls. Conf.*, Sep. 2011, pp. 1–5, doi: 10.1109/VPPC.2011.6043150.

[60] C. Depature, W. Lhomme, and A. Bouscayrol, "Teaching electric vehicle drive control using energetic macroscopic representation," in *Proc. World Electr. Vehicle Symp. Exhib. (EVS)*, Nov. 2013, pp. 17–20, doi: 10.1109/EVS.2013.6914831.

[61] R. Kumar and B. Singh, "BLDC motor driven solar PV array fed water pumping system employing zeta converter," in *Proc. IEEE 6th India Int. Conf. Power Electron. (IICPE)*, Dec. 2014, pp. 1–6.

[62] R. Kumar and B. Singh, "Grid interactive solar PV based water pumping using BLDC motor drive," in *Proc. IEEE 7th Power India Int. Conf. (PIICON)*, Nov. 2016, pp. 1–6.

[63] R. Kumar and B. Singh, "Brushless DC motor-driven grid-interfaced solar water pumping system," *IET Power Electron.*, vol. 11, no. 12, pp. 1875–1885, Oct. 2018.

[64] B. Singh and R. Kumar, "Solar PV array fed brushless DC motor driven water pump," in *Proc. IEEE 6th Int. Conf. Power Syst. (ICPS)*, Mar. 2016, pp. 1–5.

[65] S. Sashidhar and B. G. Fernandes, "A low-cost semi-modular dual-stack PM BLDC motor for a PV based bore-well submersible pump," in *Proc. Int. Conf. Electr. Mach. (ICEM)*, Sep. 2014, pp. 24–30.

[66] S. Sashidhar and B. G. Fernandes, "A novel ferrite SMDS spoke-type BLDC motor for PV bore-well submersible water pumps," *IEEE Trans. Ind. Electron.*, vol. 64, no. 1, pp. 104–114, Jan. 2017.

[67] R. V. Medeiros, J. G. S. Ramos, T. Nascimento, A. C. Lima Filho, and A. Brito, "A novel approach for brushless DC motors characterization in drones based on chaos," *Drones*, vol. 2, no. 2, p. 14, Apr. 2018, doi: 10.3390/drones2020014.

[68] A. Bosso, C. Conficoni, D. Raggini, and A. Tilli, "A computational-effective field-oriented control strategy for accurate and efficient electric propulsion of unmanned aerial vehicles," *IEEE/ASME Trans. Mechatronics*, vol. 26, no. 3, pp. 1501–1511, Jun. 2021, doi: 10.1109/TMECH.2020.3022379.

[69] Y. Park, H. Kim, H. Jang, S.-H. Ham, J. Lee, and D.-H. Jung, "Efficiency improvement of permanent magnet BLDC with Halbach magnet array for drone," *IEEE Trans. Appl. Supercond.*, vol. 30, no. 4, pp. 1–5, Jun. 2020, doi: 10.1109/TASC.2020.2971672.

[70] K.-W. Lee, D.-K. Kim, B.-T. Kim, and B.-I. Kwon, "A novel starting method of the surface permanent-magnet BLDC motors without position sensor for reciprocating compressor," *IEEE Trans. Ind. Appl.*, vol. 44, no. 1, pp. 85–92, Jan. 2008, doi: 10.1109/TIA.2007.912734.

[71] N. Kim, H. A. Toliyat, I. M. Panahi, and M.-H. Kim, "BLDC motor control algorithm for low-cost industrial applications," in *Proc. APEC 22nd Annu. IEEE Appl. Power Electron. Conf. Expo.*, Feb. 2007, pp. 1400–1405.

[72] A. G. de Castro, W. C. A. Pereira, T. E. P. Almeida, C. M. R. de Oliveira, J. R. B. A. Monteiro, and A. A. de Oliveira, "Improved finite control-set model-based direct power control of BLDC motor with reduced torque ripple," *IEEE Trans. Ind. Appl.*, vol. 54, no. 5, pp. 4476–4484, Sep./Oct. 2018, doi: 10.1109/TIA.2018.2835394.

[73] R. Khopkar, S. M. Madmi, M. Hajiaghajani, and H. A. Tohya, "A low-cost BLDC motor drive using buck-boost converter for residential and commercial applications," in *Proc. IEEE Int. Electr. Mach. Drives Conf. (IEMDC)*, Jun. 2003, pp. 1251–1257, doi: 10.1109/IEMDC.2003.1210400.

[74] A. Lelkes, J. Krotsch, and R. W. D. Doncker, "Low-noise external rotor BLDC motor for fan applications," in *Proc. Conf. Rec. IEEE Ind. Appl. Conf. 37th IAS Annu. Meeting*, Oct. 2002, pp. 2036–2042, doi: 10.1109/IAS.2002.1043812.

[75] A. Sathyan, M. Krishnamurthy, N. Milivojevic, and A. Emadi, "A low-cost digital control scheme for brushless DC motor drives in domestic applications," in *Proc. IEEE Int. Electr. Mach. Drives Conf.*, May 2009, pp. 76–82, doi: 10.1109/IEMDC.2009.5075186.

[76] J. Sun, Y. Chai, C. Su, Z. Zhu, and X. Luo, "BLDC motor speed control system fault diagnosis based on LRGF neural network and adaptive lifting scheme," *Appl. Soft Comput.*, vol. 14, pp. 609–622, Jan. 2014.

[77] Y. Su, G. Fu, B. Wan, D. Zhang, and X. Ma, "Failure analysis of Hall-effect sensors in brushless DC starter/generator," *Eng. Failure Anal.*, vol. 103, pp. 226–237, Sep. 2019.

[78] M. Aqil and J. Hur, "A direct redundancy approach to fault-tolerant control of BLDC motor with a damaged Hall-effect sensor," *IEEE Trans. Power Electron.*, vol. 35, no. 2, pp. 1732–1741, Feb. 2020.

[79] S. M. Hosseini, F. Hosseini, and M. Abedi, "Stator fault diagnosis of a BLDC motor based on discrete wavelet analysis using Adams simulation," *Social Netw. Appl. Sci.*, vol. 1, no. 11, pp. 1–13, Oct. 2019.

[80] M. Ebadpour, N. Amiri, and J. Jatskevich, "Fast fault-tolerant control for improved dynamic performance of hall-sensor-controlled brushless DC motor drives," *IEEE Trans. Power Electron.*, vol. 36, no. 12, pp. 14051–14061, Dec. 2021, doi: 10.1109/TPEL.2021.3084921.

[81] H. Park and Y. Suh, "Fault-tolerant control strategy for reduced torque ripple of independent twelve-phase BLDC motor drive system under open-circuit faults," in *Proc. IEEE Energy Convers. Congr. Expo. (ECCE)*, Oct. 2020, pp. 3370–3375, doi: 10.1109/ECCE44975.2020.9235949.

[82] H. Li, W. Li, and H. Ren, "Fault-tolerant inverter for high-speed low-inductance BLDC drives in aerospace applications," *IEEE Trans. Power Electron.*, vol. 32, no. 3, pp. 2452–2463, Mar. 2017, doi: 10.1109/TPEL.2016.2569611.

[83] M. Villani, M. Tursini, G. Fabri, and L. Castellini, "High reliability permanent magnet brushless motor drive for aircraft application," *IEEE Trans. Ind. Electron.*, vol. 59, no. 5, pp. 2073–2081, May 2012, doi: 10.1109/TIE.2011.2160514.

[84] T. Rahimi, L. Ding, S. Peyghami, M. Kheshti, F. Blaabjerg, and P. Davari, "Time domain simulation of a five-phase BLDC motor drive," in *Proc. 11th Power Electron., Drive Syst., Technol. Conf. (PEDSTC)*, Feb. 2020, pp. 1–6, doi: 10.1109/PEDSTC49159.2020.9088430.

[85] C.-L. Jeong, Y.-K. Kim, and J. Hur, "Optimized design of PMSM with hybrid-type permanent magnet for improving performance and reliability," *IEEE Trans. Ind. Appl.*, vol. 55, no. 5, pp. 4692–4701, Sep. 2019.

[86] A. Boudouda, N. Boudjerda, M. Melit, B. Nekhoul, K. E. K. Drissi, and K. Kerroum, "Optimized RPWM technique for a variable speed drive using induction motor," in *Proc. Int. Symp. Electromagn. Compat. (EMC Eur.)*, Sep. 2012, pp. 1–6.

[87] K. S. Kim, Y. G. Jung, and Y. C. Lim, "A new hybrid random PWM scheme," *IEEE Trans. Power Electron.*, vol. 24, no. 1, pp. 192–200, Jan. 2009.

[88] P.-S. Chen and Y.-S. Lai, "Effective EMI filter design method for three-phase inverter based upon software noise separation," *IEEE Trans. Power Electron.*, vol. 25, no. 11, pp. 2797–2806, Nov. 2010.

[89] F. Krall, H. Gruebler, and A. Muetze, "Analysis of the angle modulated switching strategy for use with fractional horse power BLDC motors," *IEEE Trans. Power Electron.*, vol. 36, no. 5, pp. 5460–5472, May 2021, doi: 10.1109/TPEL.2020.3028604.

[90] T. Rahimi, S. Y. Khangah, and B. Yousefi, "Reduction EMI due to di/dt and dv/dt DC and AC sides of BLDC motor drive," in *Proc. 5th Annu. Int. Power Electron., Drive Syst. Technol. Conf. (PEDSTC)*, Feb. 2014, pp. 428–433, doi: 10.1109/PEDSTC.2014.6799414.

[91] N. Mousavi, T. Rahimi, and H. M. Kelk, "Reduction EMI of BLDC motor drive based on software analysis," *Adv. Mater. Sci. Eng.*, vol. 2016, pp. 1–9, Jan. 2016, doi: 10.1155/2016/1497360.

[92] M. Perotti and F. Fiori, "Investigating the EMI mitigation in power inverters using delay compensation," *IEEE Trans. Power Electron.*, vol. 34, no. 5, pp. 4270–4278, May 2019, doi: 10.1109/TPEL.2018.2858015.

[93] Y. Chen, M. Yang, J. Long, D. Xu, and F. Blaabjerg, "A DDS-based wait-free phase-continuous carrier frequency modulation strategy for EMI reduction in FPGA-based motor drive," *IEEE Trans. Power Electron.*, vol. 34, no. 10, pp. 9619–9631, Oct. 2019, doi: 10.1109/TPEL.2019.2891572.

[94] F. Luo, X. Zhang, D. Boroyevich, P. Mattevelli, J. Xue, F. Wang, and N. Gazel, "On discussion of AC and DC side EMI filters design for conducted noise suppression in DC-fed three phase motor drive system," in *Proc. 26th Annu. IEEE Appl. Power Electron. Conf. Expo. (APEC)*, Mar. 2011, pp. 667–672.

[95] Z. Wang, K. T. Chau, and C. Liu, "Improvement of electromagnetic compatibility of motor drives using chaotic PWM," *IEEE Trans. Magn.*, vol. 43, no. 6, pp. 2612–2614, Jun. 2007.

[96] Z. Zhu, D. Howe, E. Bolte, and B. Ackermann, "Instantaneous magnetic field distribution in brushless permanent magnet DC motors—Part I: Opencircuit field," *IEEE Trans. Magn.*, vol. 29, no. 1, pp. 124–135, Jan. 1993.

[97] Z. Q. Zhu and D. Howe, "Instantaneous magnetic field distribution in brushless permanent magnet DC motors, part II: Armature-reaction field," *IEEE Trans. Magn.*, vol. 29, no. 1, pp. 136–142, Jan. 1993.

[98] Z. Q. Zhu and D. Howe, "Instantaneous magnetic field distribution in brushless permanent magnet DC motors. III. Effect of stator slotting," *IEEE Trans. Magn.*, vol. 29, no. 1, pp. 143–151, Jan. 1993, doi: 10.1109/20.195559.

[99] Z. Zhu and D. Howe, "Instantaneous magnetic field distribution in permanent magnet brushless DC motors. IV. Magnetic field on load," *IEEE Trans. Magn.*, vol. 29, no. 1, pp. 152–158, Jan. 1993, doi: 10.1109/20.195560.

[100] B. S. Rahman and D. K. Lieu, "The origin of permanent magnet induced vibration in electric machines," *J. Vibrat. Acoust.*, vol. 113, no. 4, pp. 476–481, Oct. 1991.

[101] G. Jiao and C. D. Rahn, "Field weakening for radial force reduction in brushless permanent-magnet DC motors," *IEEE Trans. Magn.*, vol. 40, no. 5, pp. 3286–3292, Sep. 2004, doi: 10.1109/TMAG.2004.832989.

[102] J. Hur, J.-W. Reu, B.-W. Kim, and G.-H. Kang, "Vibration reduction of IPM-type BLDC motor using negative third harmonic elimination method of air-gap flux density," *IEEE Trans. Ind. Appl.*, vol. 47, no. 3, pp. 1300–1309, May 2011, doi: 10.1109/TIA.2011.2128850.

[103] H. Hu, G. Cao, S. Huang, C. Wu, and Y. Peng, "Drive circuit-based torque-ripple suppression method for single-phase BLDC fan motors to reduce acoustic noise," *IET Electr. Power Appl.*, vol. 13, no. 7, pp. 881–888, Mar. 2019.

[104] R. M. Pindoriya, A. K. Mishra, B. S. Rajpurohit, and R. Kumar, "An analysis of vibration and acoustic noise of BLDC motor drive," in *Proc. IEEE Power Energy Soc. Gen. Meeting (PESGM)*, Aug. 2018, pp. 1–5, doi: 10.1109/PESGM.2018.8585750.

[105] L. Jianjun, X. Yongxiang, and Z. Jibin, "A study on the reduction of vibration and acoustic noise for brushless DC motor," in *Proc. Int. Conf. Electr. Mach. Syst.*, Oct. 2008, pp. 561–563.

[106] M. B. Trivedi and J. J. Patel, "A DSC—Based field oriented control of SPMSM to mitigate practical difficulties with low resolution sxIncremental encoder," in *Proc. Int. Conf. Comput. Power, Energy, Inf. Commun. (ICCPEIC)*, Apr. 2014, pp. 455–461.

[107] B. Wu, D. Xu, J. Ji, W. Zhao, and Q. Jiang, "Field-oriented control and direct torque control for a five-phase fault-tolerant flux-switching permanent-magnet motor," *Chin. J. Electr. Eng.*, vol. 4, no. 4, pp. 48–56, Dec. 2018.

[108] M. Sumega, P. Rafajdus, and M. Stulrajter, "Current harmonics controller for reduction of acoustic noise, vibrations and torque ripple caused by cogging torque in PM motors under FOC operation," *Energies*, vol. 13, no. 10, p. 2534, May 2020.

[109] A. G. de Castro, W. C. A. Pereira, T. E. P. de Almeida, C. M. R. de Oliveira, J. R. B. de Almeida Monteiro, and A. A. de Oliveira, "Improved finite control-set model-based direct power control of BLDC motor with reduced torque ripple," *IEEE Trans. Ind. Appl.*, vol. 54, no. 5, pp. 4476–4484, Sep. 2018.

[110] C. K. Lad and R. Chudaman, "Simple overlap angle control strategy for commutation torque ripple minimisation in BLDC motor drive," *IET Electr. Power Appl.*, vol. 12, no. 6, pp. 797–807, Jul. 2018.

[111] L. Romeral, A. Fabrega, J. Cusido, A. Garcia, and J. A. Ortega, "Torque ripple reduction in a PMSM driven by direct torque control," in *Proc. IEEE Power Electron. Spec. Conf.*, Jun. 2008, pp. 4745–4751.

[112] T. S. Singh and A. K. Jain, "Improved direct torque controlled IPM synchronous motor using variable band 12 sector control in two level inverter," in *Proc. IEEE 6th Int. Conf. Power Syst. (ICPS)*, Mar. 2016, pp. 1–6.

[113] S. S. Hakami, I. M. Alsofyani, and K.-B. Lee, "Torque ripple reduction and flux-droop minimization of DTC with improved interleaving CSFTC of IM fed by three-level NPC inverter," *IEEE Access*, vol. 7, pp. 184266–184275, 2019.

[114] W. Jiang, P. Wang, Y. Ni, J. Wang, L. Wang, and Y. Liao, "Multimode current hysteresis control for brushless DC motor in motor and generator state with commutation torque ripple reduction," *IEEE Trans. Ind. Electron.*, vol. 65, no. 4, pp. 2975–2985, Apr. 2018.

[115] T. Sheng, X. Wang, J. Zhang, and Z. Deng, "Torque-ripple mitigation for brushless DC machine drive system using one-cycle average torque control," *IEEE Trans. Ind. Electron.*, vol. 62, no. 4, pp. 2114–2122, Apr. 2015.

[116] Y. Wei, Y. Xu, J. Zou, and Y. Li, "Current limit strategy for BLDC motor drive with minimized DC-link capacitor," *IEEE Trans. Ind. Appl.*, vol. 51, no. 5, pp. 3907–3913, Sep. 2015.

[117] Z.-S. Ho, C.-M. Uang, and P.-C. Wang, "Extracting DC bus current information for optimal phase correction and current ripple in sensorless brushless DC motor drive," *J. Zhejiang Univ. Sci. C*, vol. 15, no. 4, pp. 312–320, Apr. 2014.

[118] G. Krishnan and K. T. Ajmal, "A neoteric method based on PWM ON PWM scheme with buck converter for torque ripple minimization in BLDC drive," in *Proc. Annu. Int. Conf. Emerg. Res. Areas, Magn., Mach. Drives (AICERA/iCMMD)*, Jul. 2014, pp. 1–6.

[119] Y. Lee and J. Kim, "A novel enhanced inverted PWM driving scheme for three-phase BLDC motor drive," in *Proc. IEEE Int. Conf. Consum. Electron. Asia (ICCE-Asia)*, Jun. 2018, pp. 206–212.

[120] A. Azarudeen and D. Mary, "Performance analysis of conventional and digital PWM control scheme for speed control of BLDC motor drives," in *Proc. Int. Conf. Adv. Electr. Technol. Green Energy (ICAETGT)*, Sep. 2017, pp. 69–75.

[121] K.-Y. Nam, W.-T. Lee, C.-M. Lee, and J.-P. Hong, "Reducing torque ripple of brushless DC motor by varying input voltage," *IEEE Trans. Magn.*, vol. 42, no. 4, pp. 1307–1310, Apr. 2006.

[122] V. Viswanathan and S. Jeevananthan, "Hybrid converter topology for reducing torque ripple of BLDC motor," *IET Power Electron.*, vol. 10, no. 12, pp. 1572–1587, Oct. 2017.

[123] D. Kumar, R. A. Gupta, and H. Tiwari, "Front-end zeta converter based BLDCM drive for efficient reduction of commutation current ripple using notch-filter," *Int. Trans. Electr. Energy Syst.*, vol. 30, no. 9, Sep. 2020, Art. no. e12508, doi: 10.1002/2050-7038.12508.

[124] E. Çelik and N. Öztürk, "A new fuzzy logic estimator for reduction of commutation current pulsation in brushless DC motor drives with three-phase excitation," *Neural Comput. Appl.*, vol. 31, no. S2, pp. 1125–1134, Jun. 2017.

[125] M. A. Khan, M. N. Uddin, and M. A. Rahman, "A new loss minimization control of interior permanent magnet motor drives operating with a wavelet based speed controller," in *Proc. IEEE Ind. Appl. Soc. Annu. Meeting*, Oct. 2011, pp. 1–8.

[126] M. P. Maharajan and S. A. E. Xavier, "Design of speed control and reduction of torque ripple factor in BLdc motor using spider based controller," *IEEE Trans. Power Electron.*, vol. 34, no. 8, pp. 7826–7837, Aug. 2019.

[127] K. Xia, Y. Ye, J. Ni, Y. Wang, and P. Xu, "Model predictive control method of torque ripple reduction for BLDC motor," *IEEE Trans. Magn.*, vol. 56, no. 1, pp. 1–6, Jan. 2020, doi: 10.1109/TMAG.2019.2950953.

[128] R. Ahmadi, H. Mahmoudi, and M. Aleenejad, "Torque ripple minimization for a permanent magnet synchronous motor using a modified quasi-Z-source inverter," *IEEE Trans. Power Electron.*, vol. 34, no. 4, pp. 3819–3830, Apr. 2019.

[129] A. Das and A. K. Dhakar, "Z—Source inverter based permanent magnet brushless DC motor drive," in *Proc. IEEE Power Energy Soc. Gen. Meeting*, Jul. 2009, pp. 1–5.

[130] M. Shen, J. Wang, A. Joseph, F. Z. Peng, L. M. Tolbert, and D. J. Adams, "Constant boost control of the Z-source inverter to minimize current ripple and voltage stress," *IEEE Trans. Ind. Appl.*, vol. 42, no. 3, pp. 770–778, May 2006.

[131] F. Z. Peng, M. Shen, and Z. Qian, "Maximum boost control of the Z-source inverter," in *Proc. IEEE 35th Annu. Power Electron. Spec. Conf.*, Jun. 2004, pp. 255–260.

[132] Z. Xu and M. F. Rahman, "Comparison of a sliding observer and a Kalman filter for direct-torque-controlled IPM synchronous motor drives," *IEEE Trans. Ind. Electron.*, vol. 59, no. 11, pp. 4179–4188, Nov. 2012.

[133] Z. Wang, Z. S. Xie, and Z. Guo, "A complex fuzzy controller for reducing torque ripple of brushless DC motor," in *Proc. Int. Conf. Intell. Comput.*, Berlin, Germany: Springer, Sep. 2009, pp. 804–812.

[134] Z. Xiangjun and C. Boshi, "Influences of PWM mode on the current generated by BEMF of switch-off phase in control system of BLDC motor," in *Proc. 5th Int. Conf. Electr. Mach. Syst. (ICEMS)*, Aug. 2001, pp. 579–582.

[135] K. Basu, J. S. S. Prasad, and G. Narayanan, "Minimization of torque ripple in PWM AC drives," *IEEE Trans. Ind. Electron.*, vol. 56, no. 2, pp. 553–558, Feb. 2009, doi: 10.1109/TIE.2008.2004391.

[136] Z. Goryca, S. Różowicz, A. Różowicz, A. Pakosz, M. Leśko, and H. Wachta, "Impact of selected methods of cogging torque reduction in multipolar permanent-magnet machines," *Energies*, vol. 13, no. 22, p. 6108, Nov. 2020.

[137] O. Tosun, N. F. O. Serteller, and G. Yalcin, "Comprehensive design and optimization of brushless direct current motor for the desired operating conditions," in *Proc. 25th Int. Conf. Electron.*, Jun. 2021, pp. 1–6, doi: 10.1109/IEEECONF52705.2021.9467459.

[138] A. Kumar, R. Gandhi, R. Wilson, and R. Roy, "Analysis of permanent magnet BLDC motor design with different slot type," in *Proc. IEEE Int. Conf. Power Electron., Smart Grid Renew. Energy (PESGRE)*, Jan. 2020, pp. 1–6.

[139] B. Gecer, O. Tosun, H. Apaydin, and N. F. Oyman Serteller, "Comparative analysis of SRM, BLDC and induction motor using ANSYS/Maxwell," in *Proc. Int. Conf. Electr., Comput., Commun. Mechatronics Eng. (ICECCME)*, Oct. 2021, pp. 1–6, doi: 10.1109/ICEC-CME52200.2021.9591010.

[140] M. Fazil and K. R. Rajagopal, "A novel air-gap profile of single-phase permanent-magnet brushless DC motor for starting torque improvement and cogging torque reduction," *IEEE Trans. Magn.*, vol. 46, no. 11, pp. 3928–3932, Nov. 2010.

[141] S. M. Taher, A. H. Niasar, and S. A. Taher, "A new MPC-based approach for torque ripple reduction in BLDC motor drive," in *Proc. 12th Power Electron., Drive Syst., Technol. Conf. (PEDSTC)*, Feb. 2021, pp. 1–6.

[142] M. Masmoudi, B. El Badsi, and A. Masmoudi, "DTC of B4-inverter-fed BLDC motor drives with reduced torque ripple during sector-to-sector commutations," *IEEE Trans. Power Electron.*, vol. 29, no. 9, pp. 4855–4865, Sep. 2014.

[143] M. S. Patil, R. Medhane, and S. S. Dhamal, "Comparative analysis of various DTC control techniques on BLDC motor for electric vehicle," in *Proc. 7th Int. Conf. Smart Struct. Syst. (ICSSS)*, Jul. 2020, pp. 1–6, doi: 10.1109/ICSSS49621.2020.9201982.

[144] J. Park and D.-H. Lee, "Simple commutation torque ripple reduction using PWM with compensation voltage," *IEEE Trans. Ind. Appl.*, vol. 56, no. 3, pp. 2654–2662, May 2020.

[145] U. K. Soni and R. K. Tripathi, "BLDC motor specific PCOTLC converter with active current wave shaping for torque ripple minimization," in *Proc. IEEMA Engineer Infinite Conf. (eTechNxT)*, Mar. 2018, pp. 1–6.

[146] M. N. Gujjar and P. Kumar, "Comparative analysis of field oriented control of BLDC motor using SPWM and SVPWM techniques," in *Proc. 2nd IEEE Int. Conf. Recent Trends Electron., Inf. Commun. Technol. (RTE-ICT)*, May 2017, pp. 924–929, doi: 10.1109/RTEICT.2017.8256733.

[147] A. Bosso, C. Conficoni, D. Raggini, and A. Tilli, "A computational-effective field-oriented control strategy for accurate and efficient electric propulsion of unmanned aerial vehicles," *IEEE/ASME Trans. Mechatronics*, vol. 26, no. 3, pp. 1501–1511, Jun. 2021, doi: 10.1109/TMECH.2020.3022379.

[148] A. Bosso, C. Conficoni, D. Raggini, and A. Tilli, "A computational-effective field-oriented control strategy for accurate and efficient electric propulsion of unmanned aerial vehicles," *IEEE/ASME Trans. Mechatronics*, vol. 26, no. 3, pp. 1501–1511, Jun. 2021, doi: 10.1109/TMECH.2020.3022379.

[149] A. Khazaee, H. A. Zarchi, G. A. Markadeh, and H. M. Hesar, "MTPA strategy for direct torque control of brushless DC motor drive," *IEEE Trans. Ind. Electron.*, vol. 68, no. 8, pp. 6692–6700, Aug. 2021.

[150] M. S. Trivedi and R. K. Keshri, "Evaluation of predictive current control techniques for PM BLDC motor in stationary plane," *IEEE Access*, vol. 8, pp. 46217–46228, 2020.

[151] P. Mishra, A. Banerjee, and M. Ghosh, "FPGA-based real-time implementation of quadral-duty Digital-PWM-Controlled permanent magnet BLDC drive," *IEEE/ASME Trans. Mechatronics*, vol. 25, no. 3, pp. 1456–1467, Jun. 2020, doi: 10.1109/TMECH.2020.2977859.

[152] F. Naseri, E. Farjah, E. Schaltz, K. Lu, and N. Tashakor, "Predictive control of low-cost three-phase four-switch inverter-fed drives for brushless DC motor applications," *IEEE Trans. Circuits Syst. I, Reg. Papers*, vol. 68, no. 3, pp. 1308–1318, Mar. 2021, doi: 10.1109/TCSI.2020.3043468.

[153] B. Chokkalingam, A. Yusuff, M. Tariq, and T. Bhekisiph, "Torque-ripple mitigation for BLDC using integrated converter connected three-level T type NPC-MLI," in *Proc. Int. Conf. Electr., Electron. Comput. Eng. (UPCON)*, Nov. 2019, pp. 1–6, doi: 10.1109/UPCON47278.2019.8980096.

[154] M. Salehifar, M. Moreno-Eguilaz, G. Putrus, and P. Barras, "Simplified fault tolerant finite control set model predictive control of a five-phase inverter supplying BLDC motor in electric vehicle drive," *Electr. Power Syst. Res.*, vol. 132, pp. 56–66, Mar. 2016, doi: 10.1016/j.epsr.2015.10.030.

[155] M. Perotti, "On the influence of the load parasitics on the CM conducted EMI of BLDC motor drives," in *Proc. IEEE Int. Conf. Environ. Electr. Eng. IEEE Ind. Commercial Power Syst. Eur. (EEEIC/I&CPS Eur.)*, Jun. 2020, pp. 1–6, doi: 10.1109/EEEIC/ICPSEurope49358.2020.9160663.

[156] E. Agamloh, A. von Jouanne, and A. Yokochi, "An overview of electric machine trends in modern electric vehicles," *Machines*, vol. 8, no. 2, p. 20, Apr. 2020, doi: 10.3390/machines8020020.

[157] B. Sarlioglu, C. T. Morris, D. Han, and S. Li, "Benchmarking of electric and hybrid vehicle electric machines, power electronics, and batteries," in *Proc. Int. Aegean Conf. Electr. Mach. Power Electron. (ACEMP), Intl Conf. Optim. Electr. Electron. Equip. (OPTIM) Int. Symp. Adv. Electromech. Motion Syst. (ELECTROMOTION)*, Sep. 2015, pp. 519–526.

[158] *BLDC Surface Mount*. Accessed: May 21, 2022. [Online]. Available: https://www.edn.com/brushless-dc-motors-part-i-construction-and-operating-principles/

[159] [Online]. Available: https://www.alliedmotion.com/product-overview/

[160] [Online]. Available: https://www.kdedirect.com/blogs/news/90457923-the-best-brushless-motors-for-heavy-lift

[161] [Online]. Available: https://www.electricalelibrary.com/en/2017/10/10/brushless-motors/

[162] [Online]. Available: https://www.rt.com/usa/313081-shotgun-shell-drone-shooting/

[163] *Design Evaluation Including Sizing, Optimization, Efficiency Maps*. Accessed: Jan. 9, 2022. [Online]. Available: http://emotorseng.com/recent-projects/

[164] *Rotor Laminations*. Accessed: Dec. 25, 2021. [Online]. Available: http://www.jystator.com/hpr%E2%80%930_413_15.html/stator

RANJEEV ARULDAVID received the undergraduate degree from the SRM Institute of Science and Technology, Chennai, Tamil Nadu, India, in 2021. He is currently pursuing his internship with the E-Mobility Research Centre, Department of Electrical and Electronics Engineering, SRM Institute of Science and Technology, under DST SERB Core Research Grant, File no.: CRG/2019/005483. His research interests include electric vehicle, e-motor design, motor controllers, and power converters for EVs.

RAJESH VERMA received the B.E., M.E., and Ph.D. degrees in electronics and communication engineering from MNNIT, Prayagraj, in 1994, 2001, and 2011, respectively. He has work experience of more than 20 years of teaching and administration at many reputed institutes in India, including MNNIT and many others. He also worked in telecom industry for four years at New Delhi, India. He is an Associate Professor with the Department of Electrical Engineering, King Khalid University, Abha, Saudi Arabia. His research interests include computer networks, MAC protocols, wireless and mobile communication systems, sensor networks, peer-to-peer networks, and M-2-M networks.

K. SATHIYASEKAR was born in Erode, Tamil Nadu, India. He received the B.E. degree in electrical and electronics engineering from the University of Madras, in 1999, the M.Tech. degree in high voltage engineering from SASTRA Deemed University, Thanjavur, in 2002, and the Ph.D. degree in high voltage engineering from Anna University, Chennai, India, in 2010. He is currently a Professor with the Department of Electronics and Communication Engineering, Prathyusha Engineering College, Chennai. Under his guidance, 13 scholars had completed their doctorate degree and eight others are currently pursuing the Ph.D. degree with Anna University. He has been an Expert Member for Ph.D. Viva-Voce Examination (University Nominee). He received a fund of Rs. 2.5 crores from the Ministry of MSME for Business Incubation Cell and also received fund from MNRE, Government of India, for FDP Program. He is an Editorial Board Member of the *International Journal of Advanced Research in Electrical, Electronics and Instrumentation Engineering*. He received the Award of "Certificate of Outstanding Contribution in Reviewing" from the *International Journal of Electrical Power and Energy Systems* (Elsevier, Amsterdam, The Netherlands). He received the Best Paper Award at the International Conference on Digital Factory 2008, held at CIT, Coimbatore. He is a reviewer for reputed journals, such as IEEE, Elsevier, Technical Gazette, and Australian journals.

DEEPAK MOHANRAJ received the bachelor's degree (Hons.) in electrical and electronics engineering and the master's degree in power electronics and drives from Anna University, in 2007 and 2011, respectively. He is currently pursuing the Ph.D. degree with the SRM Institute of Science and Technology, Chennai, India. He has gained 11 years of teaching experience in engineering colleges. Currently, he is doing his research work with the E-Mobility Research Centre, Department of Electrical and Electronics Engineering, SRM Institute of Science and Technology. His research interests include electric vehicle, e-motor design, motor controllers, and power converters for electric vehicles.

ABDULWASA B. BARNAWI received the B.Sc. degree in electrical power engineering from the Yanbu Industrial College, the master's degree in electrical engineering from the University of New Haven, West Haven, CT, USA, and the Ph.D. degree in electrical engineering from the Department of Electrical Engineering and Computer Science, The University of Toledo, Toledo, OH, USA. He is an Assistant Professor with the Department of Electrical Engineering, College of Engineering, King Khalid University, Abha, Saudi Arabia. His current research interests include renewable energy integration, power systems planning, generation adequacy evaluation, energy management (applying priced-based demand response strategies), smart grid, and dynamic electricity pricing such as time of use (TOU), critical peak pricing (CPP), and real-time pricing (RTP).

BHARATIRAJA CHOKKALINGAM (Senior Member, IEEE) received the Bachelor of Engineering degree in electrical and electronics engineering from the Kumaraguru College of Technology, Coimbatore, India, in 2002, the Master of Engineering degree in power electronics engineering from the Government College of Technology, Coimbatore, in 2006, and the Ph.D. degree, in 2015. He completed his first postdoctoral fellowship at the Centre for Energy and Electric Power, Faculty of Engineering and the Built Environment, Tshwane University of Technology, South Africa, in 2016, with the National Research Foundation funding. He completed his second postdoctoral fellowship with the Department of Electrical and Computer Engineering, Northeastern University, Boston, USA, where he is a Visiting Researcher Scientist. He is a Visiting Researcher with the University of South Africa. He was collaborated with leading Indian overseas universities for both teaching and research. He has completed six sponsored projects from various government and private agencies. He also singed MoU with various industries. Currently, he is running two funded research projects in wireless charging of EV and UAV under DST SERB Core Research Grant, Government of India. He is currently an Associate Professor with the Department of Electrical and Electronics Engineering, SRM Institute of Science and Technology, Kattankulathur Campus, Chennai, India. He has authored more than 110 research articles, which are published in international journal, including various IEEE TRANSACTIONS. His research interests include power electronics converter topologies and controls for PV and EV applications, PWM techniques for power converters and adjustable speed drives, wireless power transfer, and smart grid. He was the award recipient of DST and the Indo–U.S. Bhaskara Advanced Solar Energy, in 2017. He is an award recipient of the Young Scientists Fellowship, Tamil Nadu State Council for Science and Technology, in 2018.

LUCIAN MIHET-POPA (Senior Member, IEEE) was born in 1969. He received the bachelor's degree in electrical engineering, the master's degree in electric drives and power electronics, and the Ph.D. and Habilitation degrees in electrical engineering from Politehnica University Timisoara, Romania, in 1999, 2000, 2002, and 2015, respectively. From 1999 to 2016, he was with Politehnica University Timisoara. He has also worked as a Research Scientist with Danish Technical University, from 2011 to 2014; and with Aalborg University, Denmark, from 2000 to 2002. He held a postdoctoral position with Siegen University, Germany, in 2004. Since 2016, he has been working as a Full Professor in energy technology with Østfold University College, Norway. He is also the Head of the Research Laboratory "Intelligent Control of Energy Conversion and Storage Systems" and is one of the Coordinators of the master's degree program in "green energy technology" with the Faculty of Engineering, Østfold University College. He has participated in more than 15 international grants/projects, such as FP7, EEA, and Horizon 2020. He has been awarded more than ten national research grants. He has published more than 130 papers in national and international journals and conference proceedings, and ten books. His research interests include modeling, simulation, control, and testing of energy conversion systems; and distributed energy resources (DER), components, and systems, including battery storage systems (for electric vehicles and hybrid cars and vanadium redox batteries), as well as interactive buildings in smart grids. He has served as a Scientific and Technical Program Committee Member for many IEEE conferences. He was invited to join the Energy and Automotive Committees by the President and the Honorary President of the Atomium European Institute, working in close cooperation with and under the umbrella of the EC and EU Parliament; and was also appointed as the Chairperson of the AI4People, Energy Section. Since 2017, he has been a Guest Editor of five special issues of *Energies* (MDPI), *Applied Sciences*, *Majlesi Journal of Electrical Engineering*, and *Advances in Meteorology*.

• • •